Applied Energy 282 (2021) 116096

Contents lists available at ScienceDirect

Applied Energy

journal homepage: www.elsevier.com/locate/apenergy

A fundamental unified framework to quantify and characterise energy flexibility of residential buildings with multiple electrical and thermal energy systems

Adamantios Bampoulas [a,b,*], Mohammad Saffari [a,b], Fabiano Pallonetto [a], Eleni Mangina [a,c], Donal P. Finn [a,b]

[a] UCD Energy Institute, University College Dublin, Dublin, Ireland
[b] UCD School of Mechanical and Materials Engineering, University College Dublin, Dublin, Ireland
[c] UCD School of Computer Science, University College Dublin, Dublin, Ireland

ARTICLE INFO

Keywords:
Demand response
Energy flexibility
Flexibility indicators
Residential sector
Smart grid

ABSTRACT

To date, the energy flexibility assessment of multicomponent electrical and thermal systems in residential buildings is hindered by the lack of adequate indicators due to the different interpretations, properties, and requirements that characterise an energy flexible building. This paper addresses this knowledge gap by presenting a fundamental energy flexibility quantification framework applicable to various energy systems commonly found in residential buildings (i.e., heat pumps, renewables, thermal and electrical storage systems). Using this framework, the interactions between these systems are analysed, as well as assessing the net energy cost of providing flexibility arising from demand response actions where onsite electricity production is present. A calibrated white-box model of a residential building developed using EnergyPlus (including inter alia a ground source heat pump, a battery storage system, and an electric vehicle) is utilised. To acquire daily energy flexibility mappings, hourly independent, and consecutive demand response actions are imposed for each energy system, using the proposed indicators. The obtained flexibility maps give insights into both the energy volumes associated with demand response actions and qualitative characteristics of the modulated electricity consumption curves. The flexibility potential of each studied energy system is determined by weather and occupant thermal comfort preferences as well as the use of appliances, lighting, etc. Finally, simulations show that zone and water tank thermostat modulations can be suitably combined to shift rebound occurrences away from peak demand periods. These insights can be used by electricity aggregators to evaluate a portfolio of buildings or optimally harness the flexibility of each energy system to shift peak demand consumption to off-peak periods or periods of excess onsite electricity generation.

1. Introduction

Traditionally, the development of electricity markets has focused on the role of the supply side to meet demand side requirements in an effective and economic manner [1]. The widespread penetration of intermittent renewable energy sources (RES) electricity production in conjunction with the emergence of new technologies (e.g., smart metres, home automation systems, energy storage systems) has shifted attention to the role that the demand-side – in particular customers and their agents – can play to improve the operation of wholesale and retail electricity markets [1]. The definitions of demand side flexibility (DSF) vary depending on the interests of the different stakeholders involved (market-led and network-led perspectives) [2]. The definition adopted in the current paper incorporates both approaches and reads as follows: "DSF can be defined as the ability to strategically alter electricity usage by consumers (either commercial or residential) from their normal consumption profiles, by responding to control signals from grid operators and/or financial incentives from electricity generators/aggregators. The scope of these signals is to modulate and optimise electricity usage and to balance electricity production and consumption" [2]. DSF in this respect is widely recognised by policymakers and market participants as a promising resource to facilitate better efficiencies and sustainability of the electricity system at a reasonable cost. DSF can enhance energy supply security, facilitate the integration of RES, and promote market competition as well as consumer involvement [3]. With the rapid expansion of RES and a new bidding RES target of

* Correspondence to: School of Mechanical and Materials Engineering, University College Dublin, Ireland.
E-mail address: adamantios.bampoulas@ucdconnect.ie (A. Bampoulas).

https://doi.org/10.1016/j.apenergy.2020.116096
Received 21 May 2020; Received in revised form 15 October 2020; Accepted 22 October 2020
Available online 11 November 2020

32% for the European Union (EU) for 2030, increased electric system flexibility will be needed [4].

Buildings have the potential to play a key role in the future smart electricity grid as they account for approximately 40% of global energy consumption [5]. The electrification of buildings constitutes an additional reason for the onward interest in the concept of energy flexibility due to the increasing electrification of residential heating systems by using heat pumps (HP) and the ongoing adoption of distributed generation technologies, storage technologies, and electric vehicles (EVs) [6]. The IEA EBC Annex 67 has highlighted the need to harmonise building and associated energy systems engineering – both thermal and electrical – as well as occupant interaction [7]. Notwithstanding that buildings have been a widely acknowledged component of smart systems, the energy flexibility related to them lacks commonly accepted definitions and a uniform understanding mainly due to the different requirements and properties of an energy flexible building. The definition adopted by Annex 67 for the energy flexibility of buildings is as follows [8]: "the ability to manage its demand and generation according to local climate conditions, user needs and grid requirements. Energy flexibility of buildings will thus allow for demand-side management/load control and thereby demand response based on the requirements of the surrounding grids and the availability of RES to minimise the CO_2 emissions".

Aggregators and end-users (building owners and managers) are the major stakeholders interested in the energy flexibility potential of a given building. Building owners are primarily interested in energy usage and associated cost savings from activating the flexibility of specific devices, whereas aggregators may be more interested in both the broader business potential of DR, and the technical issues (building power shifting capability, response time, and maximum time a response can be maintained) to facilitate grid integration of residential building stock [9].

The dissimilarity amongst different definitions of energy flexibility of buildings [10–15] coupled with numerous flexibility quantification frameworks [12,13,16–24] gives rise to diversity of interpretations of these concepts. In the current work, building flexibility is related to the capability of a building to modify its demand, the strategies followed, and the metrics used to quantify this flexibility. Currently, the most prevalent approach to analyse flexibility is focused on given case studies by assuming specific market policies and system configurations. Previous work has mainly focused on analysing energy flexibility in an implicit manner by determining the contribution of different control schemes to achieving specific objectives, e.g., cost or/and carbon emissions minimisation, etc., [25,26]. Few studies explicitly evaluate energy flexibility by using a standardised methodology that does not depend on the underlying load control algorithms and the associated optimisation objectives [27]. The dependency on the underlying algorithms prevents electricity aggregators from accurately assessing the flexibility potential of their customers and this hampers the optimisation of their portfolios.

In contrast to the aforementioned studies, other research efforts have utilised case-independent approaches to evaluate energy flexibility; the rationale behind these studies is the development of flexibility characterisation methods by introducing generic metrics/indicators. For example, [12] quantify the flexibility of various energy systems by determining a variety of possible power modulations during a specific demand response period; however, this study focus on the flexibility used at a specific point in time without investigating associated flexibility arising from secondary or later effects (i.e., rebound effects).

Most studies that explicitly quantify the DR potential of buildings are mainly focused on heating systems and more specifically the building structural thermal mass [16,18–21,28,29]. Building mass exhibits thermal inertia by providing an opportunity to be used as a storage unit. This inherent property can be exploited to store energy either by preheating or precooling a building. Building heating or cooling systems can be used in a flexible manner depending on the utility requirements without significantly compromising the occupant thermal comfort. During non-occupancy periods this strategy has a greater potential since it allows thermal comfort constraints to be relaxed [30].

From an end-user perspective, an explicit building mass flexibility evaluation method has been proposed by [16] who originally introduced the concept of storage capacity and storage efficiency to investigate the flexibility potential of building thermal mass. The storage capacity refers to the energy that can be added to the building thermal mass during a specific DR action, whereas the storage efficiency is a measure of the energy cost associated with the specific DR action. Other studies [21,29], have extended the notions of storage capacity and storage efficiency by also considering downward regulation when quantifying the building mass flexibility potential. Similarly, in [17] energy flexibility is quantified with respect to the energy that can be added/curtailed and the associated energy savings/costs during a DR event. Other research efforts quantify flexibility offered by the building thermal mass either by calculating the amount of energy that can be shifted for a specific duration and the corresponding energy cost [28] or by introducing a flexibility indicator which assesses the capability of the building heating system to shifting its heating energy away from both high price and high load periods [19] or only high price periods [18]. Finally, in [20] flexibility is quantified in terms of load volumes shifted and in terms of procurement costs avoided during a DR action.

Moreover, it has been shown that the combination of heat pumps with thermal energy storage (TES) systems can further improve the heating system DR potential [31,32]. However, there are still outstanding challenges, particularly from an operational optimisation perspective, regarding the operational flexibility of heating systems coupled with TES. This is because, DR actions related to TES systems are accompanied by significant rebounds [31], thereby influencing the performance of the wider HVAC system, and which can compromise occupant thermal comfort [32]. Despite the ongoing interest in hot water TES system flexibility few studies develop explicit quantification methods. For instance, [33] used the indicators proposed in [16] to quantify the energy flexibility of an active TES system. The main limitation of these studies [16,33] lies in the very definitions of the adopted indicators which assess the energy shifting capability of the studied storage units by only considering upward regulation. Furthermore, [13] and [34] quantify power and energy flexibility by calculating the associated forced and delayed operation times to analyse the flexibility potential of heat pumps and combined heat and power plants when combined with thermal energy storage. [23] has extended this methodology by also considering the contribution of local RES combined with a battery storage system. Finally, flexibility in [22] is quantified in relation to the energy added/curtailed, the associated energy costs/savings with respect to the energy shifted, and a factor that determines the electricity cost during operation. In light of the foregoing, energy flexibility evaluation – both in terms of energy shifting capability and associated energy costs – has been limited to the structural thermal mass and hot water TES systems. Critically, no suitable methodology exists currently to evaluate the flexibility of different thermal and electrical systems on an integrated common basis.

Table 1 summarises all reviewed papers concisely, thereby giving a useful oversight of the supporting literature references in the current paper. Concerning flexibility evaluation from an integrated energy system perspective, which includes active and passive systems (e.g., heat pumps, passive building mass, active TES systems), in conjunction with battery-based technologies (e.g., stationary batteries and electric vehicles), a significant research gap continues to exist. This is despite the advances in battery-equipped energy management systems [35,36], and vehicle to grid technologies [37,38]. Thus, a flexibility evaluation method, which explicitly quantifies the energy shifting capability and associated costs from such an integrated energy systems perspective, has not been reported in the literature to date [39] and thus is the focus of the current paper.

Table 1
Overview of explicit flexibility quantification methods.

Ref	Description	Case study energy systems
[16] [33]	Flexibility is quantified in relation to the power shifting capability, the energy increase, and associated energy costs with respect to the energy shifted during a DR action	Passive TES Active TES
[17]	Flexibility is quantified with respect to the energy that can be added/curtailed and the associated energy savings/costs during a DR event	Passive TES
[28]	Flexibility is quantified with respect to the amount of energy that can be shifted and the corresponding energy cost during a DR action	Passive TES
[18]	Flexibility is assessed by using a flexibility indicator which quantifies the ability to shift energy consumption away from high price periods	Passive TES
[19]	Flexibility is assessed by using a flexibility indicator which quantifies the ability to shift energy consumption away from high price and high load periods	Passive TES
[20]	Flexibility is quantified in terms of load volumes shifted and in terms of procurement costs avoided during a DR action	Passive TES
[21,29]	Flexibility is quantified in relation to the energy added/curtailed, and the associated energy costs/savings with respect to the energy shifted	Passive TES
[13,34]	Flexibility is quantified in relation to the respective period during which the energy consumption can be delayed or anticipated (delayed/forced times)	Passive and Active TES
[22]	Flexibility is quantified in relation to the energy added/curtailed, the associated energy costs/savings with respect to the energy shifted and a factor that determines the electricity cost during operation	Active TES
[23]	Flexibility is quantified in relation to the respective period during which the energy consumption can be delayed or anticipated (delayed/forced times) by considering the contribution of local RES	Passive and Active TES, Batteries
[12]	Flexibility is quantified by determining a variety of possible power modulations during a DR action Passive and Active TES, EVs	

To unlock the barriers to energy flexibility assessment in residential buildings, it is important to develop a unified framework that captures not only the DR potential of multicomponent thermal and electrical systems but which quantifies it concisely and consistently. The use of a fundamental unified methodology applicable to a wide range of energy systems will facilitate the quantitative comparison across different flexibility options available in residential buildings and the evaluation of different types of building energy flexibility. In the current paper, the energy flexibility evaluation is decoupled from case-specific DR strategies and control signals and is assessed at an individual energy system level by using suitable indicators. In order to assess building energy flexibility in a holistic manner, the energy flexibility potential of various building systems – both thermal and electrical – is assessed on a common basis by also considering their possible interactions. However, when the dwelling is equipped with locally produced electricity, both the energy/cost savings and the DR potential are different. It is hence important to evaluate the flexibility of building energy systems against locally produced electricity, i.e., their self-consumption rates during modulated demand periods. This quantification framework applies to various building energy systems and gives an insight into their load shifting potential and the net energy cost of various DR actions in the context of locally produced electricity. This approach allows, not only to account for the contribution of onsite electricity generation to the energy cost of individual energy strategies, but also sets up a unified framework to quantify the flexibility of several energy systems – namely electric heating, passive thermal storage, active TES systems, electric batteries, and electric vehicles – individually or in combination. Special emphasis is given to the magnitude, the volume and duration of rebounds for all energy systems investigated.

To this end, three DR performance indicators are introduced, namely, storage capacity, storage efficiency, and self-consumption. Previous studies using these indicators [16,21,29,33] focused on quantifying the flexibility potential of thermal systems and neglect the contribution of onsite electricity generation. To this end, the definitions of these indicators are extended to consider the integrated dynamics of both thermal and electrical systems and to describe the net cost for harnessing the flexibility of each studied energy system in the context of locally produced electricity. The proposed indicators are used to acquire the daily energy flexibility mappings that can facilitate the quantitative comparison across different flexibility options available in residential buildings and the evaluation of various types of building energy flexibility.

The lack of adequate indicators impedes the accurate assessment of energy flexibility for multicomponent electrical and thermal systems in residential buildings. Existing flexibility assessment methods have been limited to the building structural thermal mass, without further analysis of the flexibility potential of other thermal and electrical systems from an integrated energy system perspective. Such electrical and thermal systems are increasingly becoming ubiquitous in new and retrofitted buildings. To address this gap, a series of novel indicators are proposed so that the energy flexibility mappings of thermal and electrical systems increasingly being found in residential buildings can be formulated. The proposed indicators can be interpreted by different energy system stakeholders with different perspectives, such as building owners and aggregators.

This paper is organised as follows: Section 2 describes the overall methodology as well as the introduced energy flexibility indicators and their customisation for the considered energy storage units. In Section 3, the case study building along with its major components is described, while in Section 4, the simulation results are presented. Finally, a discussion on the obtained results and conclusions are given in Sections 5 and 6, respectively.

2. Characterisation of energy flexibility

Three DR performance indicators have been commonly used in the literature for quantifying flexibility: storage capacity, storage efficiency, and self-consumption. Storage capacity and storage efficiency were first introduced by [16] and constitute a suitable quantification framework to evaluate the energy flexibility potential of the structural thermal mass of a building. In the current research, these indicators are extended beyond building thermal mass in order to characterise the potential of integrated flexibility perspective of various energy storage mediums, namely; passive thermal mass, active TES, battery storage systems, and EVs. Although the notion of the available storage efficiency can be deemed adequate to quantify the amount of energy that can be shifted during a DR event, the definition of storage efficiency alone cannot properly describe the net cost for activating this storage

capacity in the context of locally produced electricity. This is because the energy required from the grid has the potential to be reduced by onsite electricity generation energy at that time. Accordingly, to quantify a DR action, actual energy cost, the self-consumption during a DR action is also defined, i.e., the temporal coincidence between the additional consumption during this action and onsite electricity generation. Self-consumption may be used either to mitigate the rebound effect in downward regulation or to reduce the net energy cost of a DR action in downward regulation.

2.1. Active DR modulations and characteristics

In the context of a demand response event, the two available energy flexibility types include downward (down-flex) and upward flexibility (up-flex) [40]. In down-flex, the control setpoint is set so that the power consumption of the energy system can be reduced accordingly. In this case, energy is curtailed during the modulation period and it is restored later, in order for the considered storage medium to return to the state before the DR action. This strategy can be used for building load shaving. However, when solar energy is available during the rebound, the net energy cost of the DR action both for the customer and the utility is reduced by the corresponding solar energy amount. Fig. 1 qualitatively depicts a scenario of a down-flex when local electricity generation is available — for example, solar power, where t_{DR} is the duration of the DR event, whereas τ_{rd} and τ_{id} are the total times of the reduced and increased demand, respectively. The area A (green) corresponds to the energy reduction during the DR event, the area C (yellow) corresponds to the fraction of the rebound covered by local electricity production, the area D (orange) corresponds to the fraction of the rebound effect covered by the grid, while area B (black bold line) corresponds to the associated complete rebound energy. In up-flex, the control setpoint is suitably modulated so that energy can be stored in the storage medium. This strategy can be used for valley filling. Nevertheless, in case of coincidence between the DR action and onsite electricity generation, the actual cost of the DR event is reduced by the corresponding solar energy amount. Likewise in Fig. 2, an up-flex scenario is depicted; the energy increase corresponds to the area B (black bold line), the electricity purchased from the grid corresponds the area D (orange), the electricity covered by local generation corresponds to the area C (yellow), and the area B (green) corresponds to the energy decrease (inverse rebound) related to this event.

2.2. Energy flexibility indicators

Three flexibility indicators can be defined for the down-flex and up-flex type DR actions (self-consumption, storage capacity, and storage efficiency).

2.2.1. Self-consumption during DR action

The self-consumption during a DR action (SC_{DR}) is defined as the proportion of increased demand covered by onsite generation. This indicator is a measure of the coincidence between locally produced electricity and increased demand during a DR action. In down-flex, the demand increases during the rebound, while in up-flex, the demand increases during the DR action. SC_{DR} both for down-flex and up-flex is given by Eq. (1).

$$SC_{DR} = \frac{C}{C+D} = \frac{\int_0^{\infty} (\max(\min(P_{\mathrm{mod}}, P_{RES}) - \mathrm{P}_{ref}), 0)dt}{\int_0^{\infty} (P_{\mathrm{mod}} - \mathrm{P}_{ref})^{+}dt} \quad (1)$$

Where the "+" and "-" superscripts are interpreted as follows:

$$x^{+} = max(x, 0) \quad , \quad x^{-} = max(-x, 0)$$

and P_{mod} and P_{ref} stand for the total modulated and reference building load, respectively, while P_{RES} is the onsite electricity generation.

2.2.2. Storage capacity

In this study, the available storage capacity (C_{DR}) of an energy storage medium is defined as the amount of energy that can be added to or removed from the storage system during an active DR action without violating the defined boundary conditions. In down-flex, the storage capacity corresponds to the area A of Fig. 1 and it is given by Eq. (2). In up-flex, the capacity of a storage medium is depicted by the area A of Fig. 2; however, since locally produced electricity is usually uncontrolled, the impact of specific DR events in terms of net energy purchase can be only assessed by also considering the temporal coincidence between demand increase and onsite electricity production. In this sense, the net energy purchase from the utility corresponds to the area D of Fig. 2 and is given by Eq. (3). It should be noted that Eq. (3) resolves to Eq. (4), when $P_{RES} = 0$.

$$A = C_{DF} = \int_0^{\infty} \left| (P_{\mathrm{mod}} - \mathrm{P}_{ref})^{-} \right| dt \quad (2)$$

$$D = C_{UF}^{net} = (1 - SC_{DR})C_{UF} = \int_0^{\infty} \max(P_{\mathrm{mod}} - \max(\mathrm{P}_{ref}, P_{RES}), 0)dt \quad (3)$$

$$A = C_{UF} = \int_0^{\infty} (P_{\mathrm{mod}} - \mathrm{P}_{ref})^{+}dt \quad (4)$$

2.2.3. Storage efficiency

The activation of an energy storage medium results in a different power demand after the end of the DR action. In case of down-flex, the demand is expected to increase, whereas in case of up-flex, this demand is expected to decrease. Depending on the storage medium and its control characteristics, such rebounds may occur immediately after the DR action or they can be postponed by applying suitable control strategies. Regardless of the rebound occurrence time, in the current research, they are quantified by applying the same methodology. Nevertheless, the interpretation of storage efficiency is different in downward and upward flexibility due to the different control associated strategies.

- Storage Efficiency in down-flex
  In down-flex, storage efficiency is defined as the fraction of the energy cost of an active DR event with respect to the energy reduction achieved during this event. The storage efficiency of a down-flex scenario η_{DF} is calculated as per equation (5):

$$\eta_{DF} = 1 - \frac{D}{A} = 1 - (1 - SC_{DR})\frac{B}{A} = \\ = 1 - \frac{\int_0^{\infty} \max(P_{\mathrm{mod}} - \max(\mathrm{P}_{ref}, P_{RES}), 0)dt}{\int_0^{\infty} \left| (P_{\mathrm{mod}} - \mathrm{P}_{ref})^{-} \right| dt} \quad (5)$$

  This indicator ranges between 0 and 1 and depends, not only on the relationship between the energy cost and the curtailed energy amount, but also on the coincidence between the rebound and the locally produced electricity. For example, for smaller energy costs and higher self-consumption rates, the efficiency increases.
- Storage Efficiency in up-flex
  In up-flex, storage efficiency is defined as the fraction of the energy that is consumed during an active DR event and can be subsequently used to reduce the power needed to restore the previous control setpoints. The storage efficiency in an up-flex scenario is given by Eq. (6).

$$\eta_{UF} = \frac{B}{D} = \frac{B}{(1 - SC_{DR})A} \quad (6)$$

  However, this formula can be infinite if all the energy spent during the DR action is covered by locally produced electricity. Thus, Eq. (6) is suitably transformed so that storage efficiency ranges between 0 and 1. The updated storage efficiency is given by Eq. (7).

$$\eta_{UF} = \frac{B}{B + (1 - SC_{DR})A} = \\ = \frac{\int_0^{\infty} \left| (P_{\mathrm{mod}} - P_{ref})^{-} \right| dt}{\int_0^{\infty} \left| (P_{\mathrm{mod}} - P_{ref})^{-} \right| dt + \int_0^{\infty} \max(P_{\mathrm{mod}} - \max(\mathrm{P}_{ref}, P_{RES}))dt} \quad (7)$$

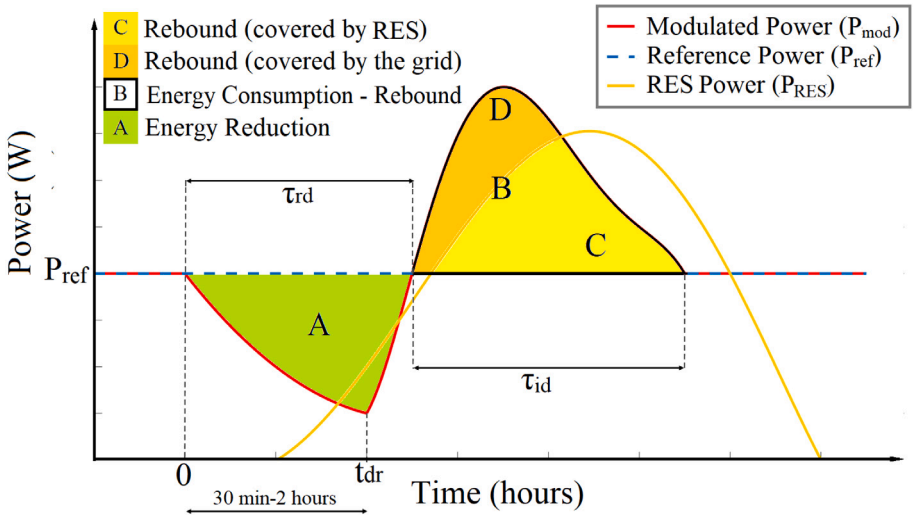

Fig. 1. Down-Flex action.

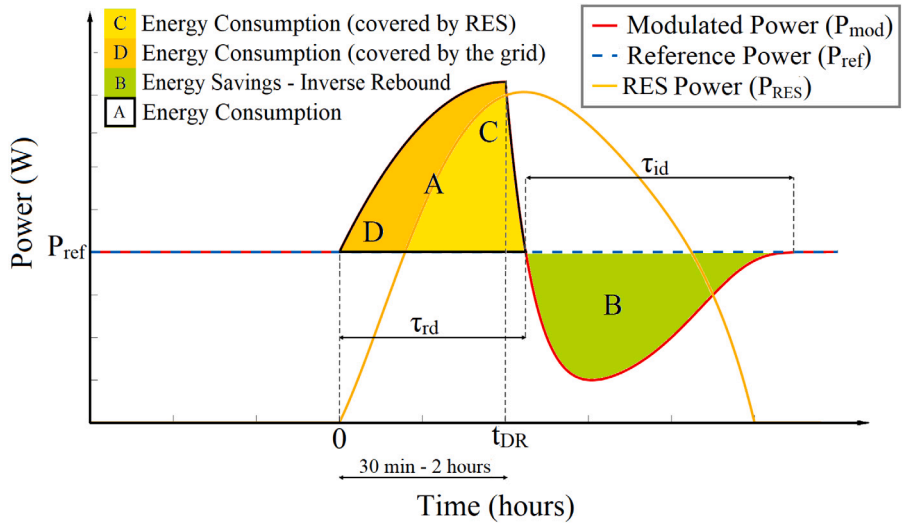

Fig. 2. Up-Flex action.

2.3. Methodology implementation for different energy systems

The application of the previous indicators (Eqs. (1)–(7)) is analysed and extended for additional energy systems that may be present in a building when considering flexibility. The energy flexibility assessment concerns structural (passive) TES, active TES, as well as electrical energy storage systems (stationary battery and EV battery).

2.3.1. Structural thermal energy storage

The evaluation of the structural TES flexibility potential is based on the modulation of the room thermostat setpoint (ΔT_r) for a duration of t_{DR}. In order for DR actions not to jeopardise occupant thermal comfort, the operative temperature change should lie within acceptable limits, such as those established by ASHRAE [41]. The maximum downward or upward flexibility that can be harnessed from structural TES systems are specified in Table 2. It should be noted that the associated boundary conditions could be tightened or relaxed on the basis of occupant thermal preferences.

2.3.2. Active thermal energy storage

The DR potential of a TES system is harnessed by changing its thermostatic setpoint (ΔT_s) for a duration of t_{DR}. When a TES system is coupled with the heating system, DR actions can, not only affect the hot water availability, but also the heating system performance. Therefore, the acceptable limits of ΔT_s for a given t_{DR} are case-specific and can be only determined by a heuristic analysis.

Table 2
Limits on temperature drifts and ramps [41].

Time period	0.5 h	1 h	2 h
Maximum allowed operative temperature change	1.1 °C	2.2 °C	2.8 °C

2.3.3. Electrical energy storage

Electrical energy storage in a residential building either refers to stationary batteries or batteries embedded in plug-in EVs. The direct flexibility quantification of electrical energy storage is challenging since it strongly depends on the underlying control algorithms. In both cases, the maximum flexibility potential of a DR action can be determined by considering zero power flow to the utility. In other words, the battery can only cover the local power demand, thus, it can be suitably discharged to nullify the power flows from the grid. Consequently, the battery discharging power is equal to the difference between the building load and the local RES production. When the latter is higher

than the building load, the battery remains inactive. Since battery loads can be controlled by inverter-based systems, the energy consumed or generated by a battery can be easily determined. In this sense, only downward flexibility is considered for electrical energy storage units. The use of the battery as a flexibility source comes at a cost, due to efficiency losses in charging, discharging, in the inverter and parasitic losses. These losses can be reflected in the storage efficiency; the rebound, in this case, is the restoration of the State of Charge (SoC) before the DR action. This implies that the rebound resulting from harnessing the DR potential of a battery can occur at a later time, as determined by the control algorithm. It is worth mentioning that since the battery charging power can be controlled, the rebound duration can be controlled as well. However, charging and discharging batteries exclusively from the grid is generally an unattractive solution because of the energy losses related to their charge cycle [42]. To this end, battery-based technologies are usually coupled with distributed generation (e.g., solar PV panels).

To calculate the maximum flexibility potential of a stationary battery, it is considered that it remains inactive during the baseline case at a reference SoC, SoC_{ref}. Its flexibility potential is harnessed by discharging it for a duration of t_{DR} with a power equal to the overall building load, P_b reduced by the onsite electricity generation P_{RES}. Thus, the storage capacity is calculated by customising equation (2). Eq. (2) can be further simplified by considering that $t_{DR} = \tau_{rd}$ because of the fast dynamics of the battery. During a DR period, the total building load should be equal to zero, $P_{mod} = 0$ and the baseline power is equal to the overall building load, P_b reduced by the onsite electricity generation P_{RES}, $P_{ref} = max(P_b - P_{RES}, 0)$.

$$\begin{aligned} C_{DF} &= \int_0^{\infty} \left|(P_{\mathrm{mod}} - \mathrm{P}_{ref})^-\right| dt = \\ &= \int_0^{\infty} \left|(0 - \max(P_b - P_{RES}, 0))^-\right| dt = \\ &= \int_0^{t_{DR}} \max(P_b - P_{RES}, 0) dt \end{aligned} \tag{8}$$

Considering average discharging and charging efficiencies of η_d and η_c, respectively, the energy harvested from the battery to cover C_{DF} is C_{DF}/η_d. Likewise, to recharge the battery to the previous SoC, the battery should absorb C_{DF}/η_d, thus the power purchased from the grid is $C_{DF}/\eta_d\eta_c$. Considering that the rebound commencement is t_c and τ_{rd} and τ_{id} are the total times of the reduced and increased demand, respectively, Eq. (5) can be written as follows[1]:

$$\begin{aligned} \eta_{DF} &= 1 - \frac{\int_0^{\infty} \max(P_{\mathrm{mod}} - \max(\mathrm{P}_{ref}, P_{RES}), 0) dt}{\int_0^{\infty} \left|(P_{\mathrm{mod}} - \mathrm{P}_{ref})^-\right| dt} = \\ &= 1 - \max\left(\frac{1}{\eta_c\eta_d} - \frac{1}{C_{DF}} \int_{t_c}^{t_c+\tau_{id}} \max(\mathrm{P}_b, P_{RES}) - P_b dt, 0\right) \end{aligned} \tag{9}$$

In contrast to thermal loads, in batteries, the coincidence between locally produced electricity and associated rebounds can be controlled by modulating the rebound starting time and duration. Therefore, for each DR action, different mappings of storage efficiency can be derived for all rebounds occurring in all intervals $[t_c, t_c + \tau_{id}]$ as per Eq. (9). If the rebound is scheduled during a period of zero excess electricity from onsite generation, the resulting storage efficiency becomes negative and equal to $1\text{-}1/(\eta_c\eta_d)$. Hence, it is important to implement suitable control actions to ensure optimal battery recharging from local generation.

On the other hand, an EV is a power resource only available when it is parked and plugged in. The maximum flexibility potential of an EV battery during a DR action for a duration of t_{DR} can be harnessed by considering both charging curtailment and covering the building load. In this sense, the assessment of the flexibility potential of an EV battery is similar to the methodology followed for stationary batteries.

[1] The mathematical proof can be found in the Appendix.

Fig. 3. 3D rendering and picture of testbed house [47].

3. Case study

To exemplify the use of the outlined flexibility indicators, the proposed methodology is considered for an existing all-electric house located in eastern Ireland. A white-box model, used to develop and analyse the DR control algorithms [43], was created using EnergyPlus V9.1 [44]. The analysis is based on the heating season, which extends from 01 September to 30 April.

3.1. Building model

The building and the associated modelled geometry are shown in Fig. 3. The building model was calibrated using measured data from the building with an hourly resolution according to ASHRAE guidelines [45]. The accuracy of the calibrated building model was evaluated by using the Mean Bias Error (MBE) and the Cumulative Variation Root Mean Squared Error (CVRMSE) [46]. The thermal envelope, the ground source heat pump, the PV plant, and EV were calibrated to meet the ASHRAE criteria [45]. In the following subsections, five energy systems of the building are described, as follows: building physics, HVAC system, PV system, electric vehicle, stationary battery.

3.1.1. Building description and thermal properties

The test-bed house is a single-storey building and exhibits significant passive TES capacity arising from its construction, which consists of a two-leaf concrete wall with cavity insulation. This dwelling type is classified as a detached house which represents 40% of the Irish building stock [48] and is the most common single building category [49]. The roof is covered with slate and does not have insulation, whereas the ceiling is covered with acoustic tiles to ensure both acoustic and thermal insulation. On top of the acoustic tiles, a 200 mm layer of fibreglass ensures high thermal resistance due to its low thermal conductivity (0.04 W/mK). The overall window to wall ratio is 15%, with a 22% and 10% ratio on the south and north facades, respectively. As illustrated in Fig. 4, the house consists of twelve rooms and an unused attic space at roof level. Its fabric specifications and architectural characteristics are outlined in Table 3. The heat capacities, as presented in Table 3, are calculated based on the weighted average of the interior ceiling, the exterior/interior walls, and the exterior/interior floor. The heat capacities of the aforementioned building elements are calculated by considering the specific heat capacity, the thickness, and the density of each constituent layer. The calibration of the thermal envelope was performed over an extended period during occupant absence [50]. Both the MBE and the CVRMSE were below the hourly ASHRAE standards and exhibited average values of 4.41% and 3.28%, respectively.

3.1.2. HVAC system

The space heating system consists of a variable capacity ground source heat pump (GSHP) which has a maximum rated thermal output of 12 kW. The heat pump uses as a heat source, water from a nearby ground source. As illustrated in Fig. 5, the GSHP is equipped with a hot

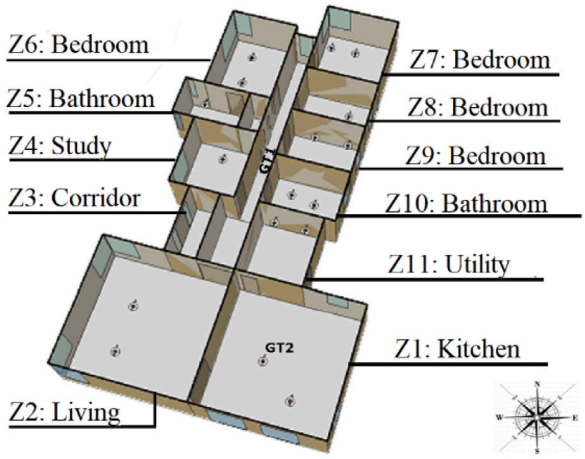

Fig. 4. Representation of the building with the ground floor thermal zones and orientation [51].

Table 3
U-Values, heat capacities with respect to element surface area, and geometrical characteristics of the building.

Building element	U-Value (W/m^2K)	Heat capacities (kJ/m^2K)	Area (m^2)
Walls	0.21	298.76	187
Roof	0.21	76.41	279
Windows	1.17	–	33
Floor	0.21	116.58	208

Table 4
Thermostatic setpoints.

Time slots	Household state	Thermostat setpoints
23:10–06:40	Non-active	16
06:40–08:20	Active	20
08:20–18:10	Absent	16
18:10–23:10	Active	21

water storage tank of 0.8 m^3, which provides an active thermal energy storage system. Control of the GSHP can be affected either by the room thermostat setpoint T_r or the water tank thermostat setpoint T_{wt}. Since ground source temperature changes were observed to be relatively small over the year (between 6 °C and 8 °C), the GSHP coefficient of performance (COP) mainly depends on the water tank temperature. Fig. 6 illustrates the COP as a function of the ground source temperature for various water tank temperatures. Lower water tank temperature setpoint and higher ground source temperatures result in higher COP; nevertheless, the latter has minor influence on the COP compared to the water tank temperature setpoint. This feature gives an additional advantage to the heating system since its overall performance can be controlled and optimised with respect to the prevailing weather conditions. The calibration was based on data from the heating season and resulted in average CVRMSE and MBE values of 3.78% and −0.61%, respectively. The adopted thermostatic setpoint is based on a daily average occupancy profile resulting from the Time Use Survey 2014–2015 (UK 2015 TUS) [52]. The considered occupancy profile uses one of the clusters deriving from categorising the household weekday diaries and represents 23% of the survey sample [53]. This cluster is characterised by a working hour absence (from 08:20 h to 18:10 h) and considers all types of occupant activity, i.e., non-active, active, absent. The room thermostat setpoints are given in Table 4 and the occupancy schedule as well as the level of activity are illustrated in Fig. 7.

3.1.3. PV system

The electrical installation includes a south facing PV system located 30 metres from the house. The 30 solar panels each have a nominal power of 200 Wp each, or 6 kWp overall. The PV system is connected to the grid through a single-phase inverter with a potential efficiency of 95%. The calibration was performed by using data for the months February through September and exhibited an average MBE of 3.6% and a CVRMSE of 12.5%, which meets the ASHRAE criteria.

3.1.4. Electric vehicle

The EV considered is a Nissan Leaf with a 24 kWh battery pack which is used for commuting of approximately 50 km per day which corresponds to 44% of its autonomy range [54]. The EV is assumed to be plugged in every day at 18:10 h and unplugged at 08:20 h . The inverter maximum charging power is 3.3 kW with an efficiency of 84% and the charging duration is approximately 4 h . The calibrated model was compared to the monitored data exhibited an annual MBE of +/- 3.5% and CVRMSE of 10.4%.

3.1.5. Stationary battery

The existing house is not equipped with electrical energy storage. In the current study, a stationary battery is incorporated in the analysis for completeness. It has a capacity of 12 kWh, a maximum charging/discharging power of 8 kW, and a two-way charging efficiency of 85%.

3.2. Consumer electricity profile

The energy flexibility assessment of the test dwelling is carried out by implementing a statistical analysis. The analysis was based on the heating periods of three years (06/2016–05/2019) by using the associated daily Heating Degree Days (HDD) to extract the most representative days of the heating season. The meteorological daily data were ordered in terms of the HDD and was ranked by using a percentile approach [55]. The HDD were calculated with respect to the prevailing weather data by considering a base temperature of 15.5 °C and were grouped into four categories. Finally, a representative day for each category was selected based on the pertinent median day.

A parametric analysis showed that thermal comfort during the coldest days of the heating season (Categories 1 and 2 - Table 5) could be only achieved when the water tank storage temperature (T_{wt}) is set to its maximum, i.e., 55 °C. However, thermal comfort can be maintained using reduced storage tank temperatures for the lower demand categories (3 and 4) as illustrated in Table 5 [56]. Given that the GSHP COP depends on this setpoint, the overall performance of the heating system can be controlled accordingly. As a result, for a specific day and thermostatic setpoints, there is a minimum storage tank temperature, $T_{wt,min}$ for which thermal comfort conditions can be maintained. Table 6 summarises the HDD category ranges, the daily heat demand ranges, the frequency of each category, the median HDD value, the total energy consumption of the selected representative day, the minimum water tank temperature, and a characterisation of the heat demand.

3.3. Energy flexibility mapping

To create the energy flexibility mapping for the four representative heat demands selected, consecutive and independent DR events are imposed, over a 24 h period, on the dwelling for each of the demand categories outlined in Table 5. The starting times of the DR strategies were based on an on-the-hour basis, i.e., 00:00 h, 01:00 h, etc. The daily number and duration of the DR actions is indicative and may vary depending on the building characteristics and energy systems, as well as the control objectives. These simulations result in the formulation of the energy flexibility profiles; which can be used to select the most suitable DR strategies, either independently or in combination, in terms of the requested energy amount (to be curtailed or increased) and the associated energy cost.

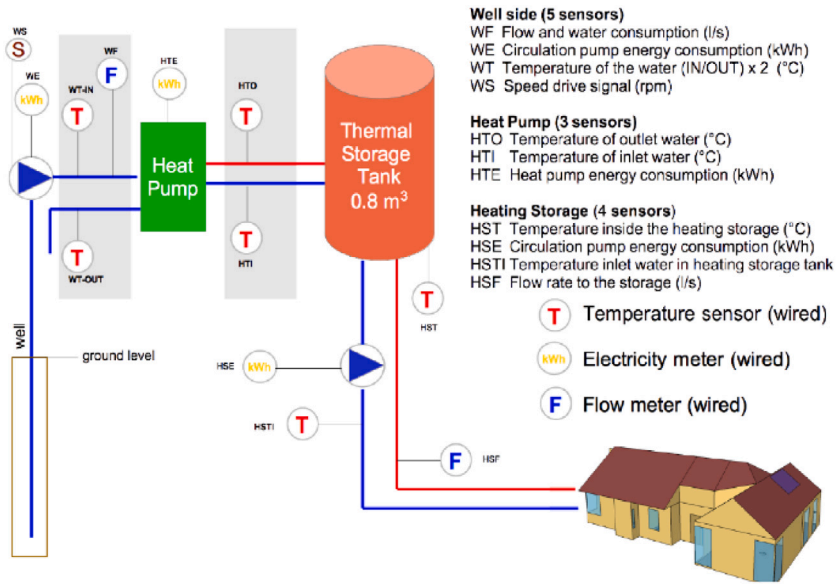

Fig. 5. Heat system design and sensor metring.

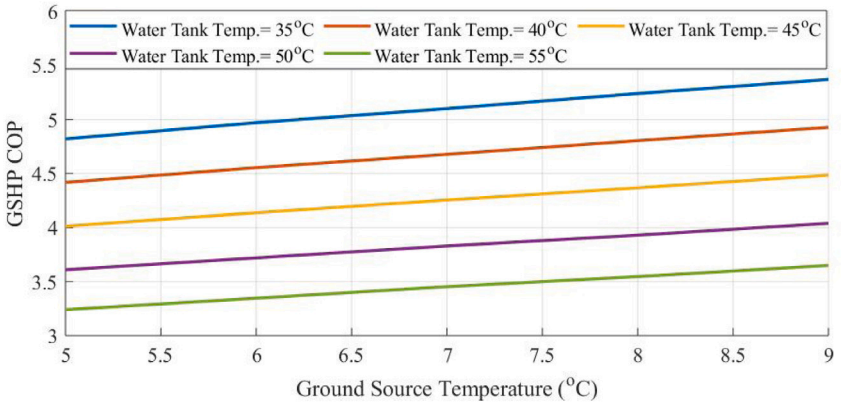

Fig. 6. GSHP COP performance map.

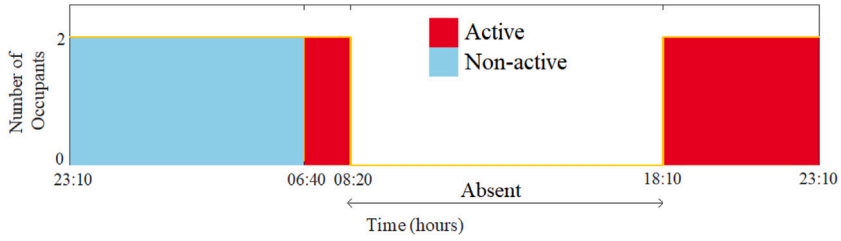

Fig. 7. Occupancy schedule and level of activity.

Table 5
Selected representative days and associated energy consumption based on 2016–2019 HDD data.

Cat.	HDD range	Daily heat demand range (kWh)	Freq. (%)	Median HDD value	Energy cons. (Rep. day) (kWh)	Min. water tank temp. (°C)	Space heating demand
1	13–17.0	0.26–16.25	8.5	14.95	22.7	55	High
2	9–12.99	4.27–20.29	34.7	10.37	17.36	55	Medium-High
3	5–8.99	8.35–23.92	37.2	6.67	13.64	45	Medium-Low
4	0–4.99	14.6–27.8	19.5	3.02	6	39	Low

Table 6
Heat demand, outdoor temperature range, water tank temperature, and daily energy consumption for each case.

Cat.	Case	Heat demand	Ambient temp. range (°C)	Storage tank temp. setpoint (°C)	Space heating energy cons. (kWh)
1	H55	High	−4.2–5.6	55	22.77
2	MH55	Medium-High	4.8–6.4	55	17.36
3	ML55	Medium-Low	7–12.4	55	13.64
	ML45	Medium-Low	7–12.4	45	10.39
4	L55	Low	10–17	55	6
	L39	Low	10–17	39	3.82

3.4. Reference cases

To evaluate the energy flexibility potential of the testbed, six different baseline cases are considered, each based on the selected representative days and the water tank temperature setpoints. Considering the representative days of Categories 1 and 2 (Table 5), the thermostatic setpoints (Table 4) can be only achieved for a water tank temperature equal to 55 °C . Thus, for each of the High and the Medium-High heat demand days, only one case is considered, H55 and MH55, respectively. However, for the representative days of Categories 3 and 4 (Table 5), thermal comfort can be maintained with different water tank temperatures (55, 45, 39 °C). For each of the Medium-Low and Low heat demand day categories, two different baselines are considered for each, by setting the water tank temperature to its maximum (ML55 and L55 cases, respectively) and by setting the water tank temperature to the permissible minimum ($T_{wt,min}$), i.e., 45 °C and 39 °C (ML45 and L39 cases, respectively). Table 6 summarises the characteristics of each of the six cases examined, including the space heat energy consumption.

Fig. 8 illustrates the building power demand and self-generation for the six baseline cases presented in Table 6. The presented load profiles are as follows: (i) the building baseload, excluding the GSHP (blue), (ii) the GSHP (black and grey), (iii) the EV (green), and (iv) the PV power generation. The room thermostat setpoint is given in Fig. 8a. The profiles are categorised according to the H55 (Fig. 8b), MH55 (Fig. 8c), ML55 and ML45 (Fig. 8d), and L55 and L39 cases (Fig. 8e). It should be noted that thermal comfort is achieved for all cases. The water tank setpoint temperature adjustment exhibits a significant energy saving potential for the ML45 case compared to the ML55 case, as well as the L39 case relative to the L39 case, as evident in the figure and Table 6. In addition, it can be observed that the higher the TES thermostatic setpoint, the greater the electricity consumed for different water tank baseline temperatures. Since the produced PV energy coincides with the lowest daily building demand (due to the reduced room thermostat setpoints during the non-occupancy period), it is important to assess the building flexibility with a view to determine its capability to shift peak consumption during periods of higher PV electricity generation.

3.5. Boundary conditions

The energy flexibility arising from the GSHP can be either harnessed by activating the passive building thermal mass or the active TES system, by modulating the respective setpoint temperatures: room temperature (T_r) and water tank TES temperature (T_{wt}). To calculate the maximum flexibility potential of each strategy, different modulation control algorithms are implemented. The passive TES flexibility is exploited by considering zone temperature setpoint step changes of +/- 2.2 °C , which correspond to the maximum allowed operative temperature changes as per ASHRAE guidelines [41] (Table 2). For the active TES system, a parametric analysis was carried out to determine the maximum T_{wt} for which thermal comfort was not violated for each of the hourly DR actions. By considering a water tank setpoint temperature reduction of $\Delta T_{wt} = 10$ °C , the maximum water tank temperature changes and the corresponding indoor operative temperature drifts were calculated during the hourly down-flex actions. The maximum water tank and room temperature drifts for all cases considered were −5.8 K and −0.45 K, respectively. This indicates that thermal comfort was not violated during hourly water tank temperature modulations because of its high thermal inertia.

The energy flexibility potential of the passive TES can be further increased by relaxing the boundary conditions during the non-occupancy periods. Specifically, during the period 08:20–18:10, the allowable thermostatic changes can be increased without affecting thermal comfort. Thus the considered temperature drifts for all hourly setpoint modulations during the non-occupancy period (08:00–09:00, 09:00–10:00,. . . , 17:00–18:00) were set equal to +/-5 °C . The methodological steps of this study are summarised in Table 7.

4. Results

In this section, the downward and upward flexibility potential of the various building energy systems is evaluated using the proposed indicators.

4.1. Downward flexibility

To investigate the impact of down-flex actions in terms of their energy shifting capability, energy cost, and coincidence with onsite electricity generation, the concepts of storage capacity, C_{DF} (Eq. (2)), storage efficiency, η_{DF} (Eq. (5)), and self-consumption, SC_{DR} (Eq. (1)) are all evaluated, as outlined in Section 2.2. The analysis considers the relevant boundary conditions, the modulated energy consumption curves, and the energy flexibility mappings.

4.1.1. Modulated energy consumption curves

The impact of rebounds on the downward flexibility potential is illustrated in Fig. 9 for a one hour demand response event for the GSHP. Modulation occurs at 07:00 h and two separate response profiles are presented. Fig. 9a(i) and (ii) examine the case where the TES tank response (MH55 case) is considered, whereas Fig. 9b(i) and (ii) examine the case where a single zone (living room — see Fig. 4) is analysed. The power deviation curves depicted in Fig. 9a (ii) and 9b (ii) result from the difference between the baseline and modulated GSHP curves depicted in Fig. 9a(i) and 9b(i), respectively. Rebounds resulting from the TES tank temperature modulation have a higher magnitude (up to 2 kW) and shorter duration (from 08:05 h to 10:20 h) compared to room thermostat setpoint modulations; the latter exhibits a maximum rebound equal to 32 W and a duration of approximately 6 h (from 10:00 h to 16:00 h). This means that rebounds resulting from each modulation can be effectively covered by specific renewables depending on their electricity production profile.

4.1.2. Energy flexibility maps

The storage capacity (C_{DF}) (Eq. (2)), resulting from the activation of the active and passive TES, as well as the stationary battery and the EV, for all hourly DR events, is presented in Fig. 10 for the H55 and MH55 cases. All hourly DR actions are assumed to be independent.

The passive TES (see Fig. 10a) exhibits lower storage capacity during occupancy periods for the H55 case, compared to the MH55 case, as a result of the limited flexibility margin; this is because thermal comfort constraints, in combination with high thermostatic setpoints and low ambient temperature, impose an upper limit on curtailment of the heating system consumption. During periods of occupant absence, thermal comfort constraints can be relaxed further; however, additional reduction of the room thermostat setpoints (as per ASHRAE guidelines [41]) does not affect the storage capacity, because the room temperature does not change beyond the maximum allowable temperature drift, i.e., 2.2 °C . Higher baseline thermostatic setpoints are associated with higher flexibility potential. The increase in flexibility is due to the additional GSHP consumption during the active occupancy periods (06:40 h –

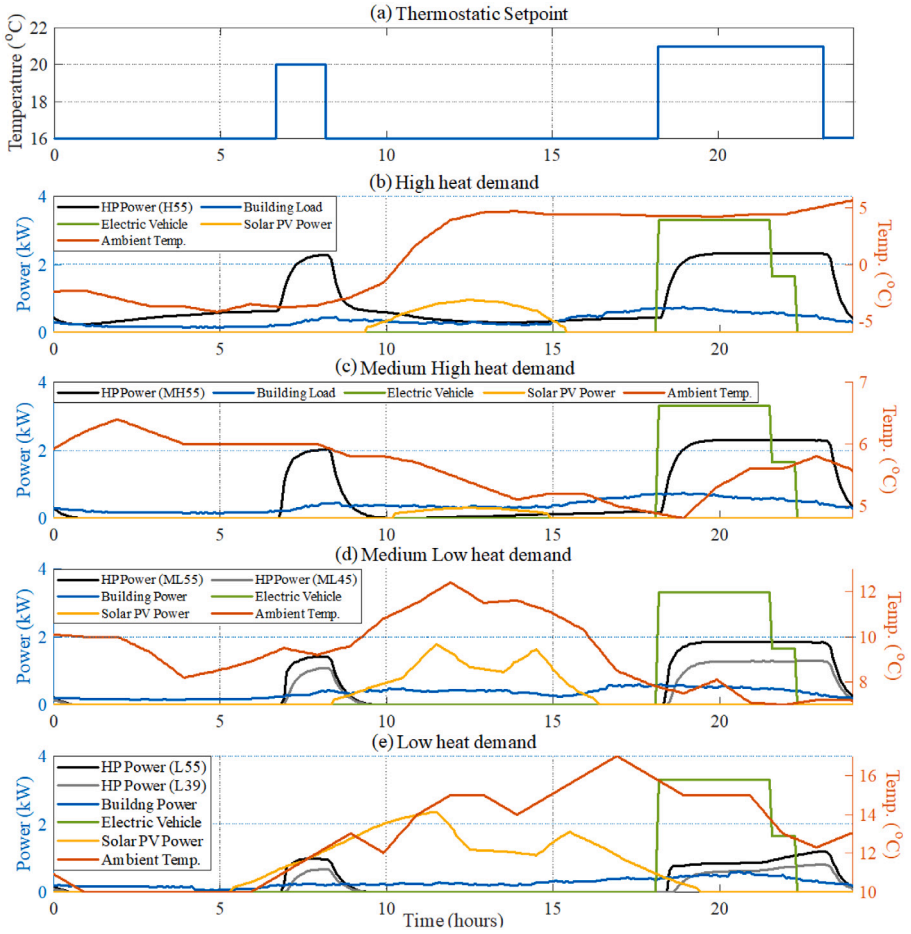

Fig. 8. Power demand profiles: Building Load (excluding HP), HP, EV and PV: (a) Room Thermostat Setpoint, (b) High, (c) Medium-High, (d) Medium-Low, (e) Low space heat demand categories.

Table 7
Methodology diagram.

Step 1	Consider a calibrated all-electrical smart grid ready residential building model			
Step 2	Select the most representative days of the heating season based on the HDDs (Table 5)			
Step 3	Consider various cases for each representative day based on the $T_{wt,min}$ (Table 6)			
Step 4	For all energy systems considered: Impose hourly independent DR actions both for down-flex and up-flex subject to the respective boundary conditions			
	Starting times: 00:00,01:00,...23:00			
Step 5	Evaluate the flexibility potential by using the following indicators:			
		Passive and Active TES		Electrical Energy Storage
		Down-Flex	Up-Flex	Down-Flex
	Storage Capacity	Eq. (2)	Eq. (4)	Eq. (8)
	Storage Efficiency	Eq. (5)	Eq. (7)	Eq. (9)
	Self-Consumption	Eq. (1)		
Step 6	Create the daily flexibility profile for all cases in Step 4 by using the indicators in Step 5			

08:20 h and 18:10 h – 23:10 h). Furthermore, it can be observed that the activation of the passive TES results in lower storage capacity compared to the active TES (see Fig. 10b), during active occupancy periods. In contrast to room thermostat modulations, the activation of the active TES has a limited impact on thermal comfort. Thus, the activation of the active TES results in higher flexibility potential for the H55 case due to the higher GSHP consumption (as a result of the lower outdoor temperature).

Considering the stationary battery (see Fig. 10c), it is discharged to cover the building load, the energy provided by the battery depends on the difference between the building electrical load and PV generation. Thus, during periods of high solar irradiance, the storage capacity (C_{DF}) (Eq. (8)) is zero. On the contrary, when the zone thermostat setpoint is higher, the battery storage capacity increases due to the higher GSHP power consumption. The stationary battery storage capacity is lower for the H55 case from 11:00 h to 15:00 h , because of the higher PV generation.

The EV (see Fig. 10d) can only offer flexibility when it is plugged in. The EV and the stationary battery storage capacity profile are broadly similar, except for the EV charging period; during that period, the EV

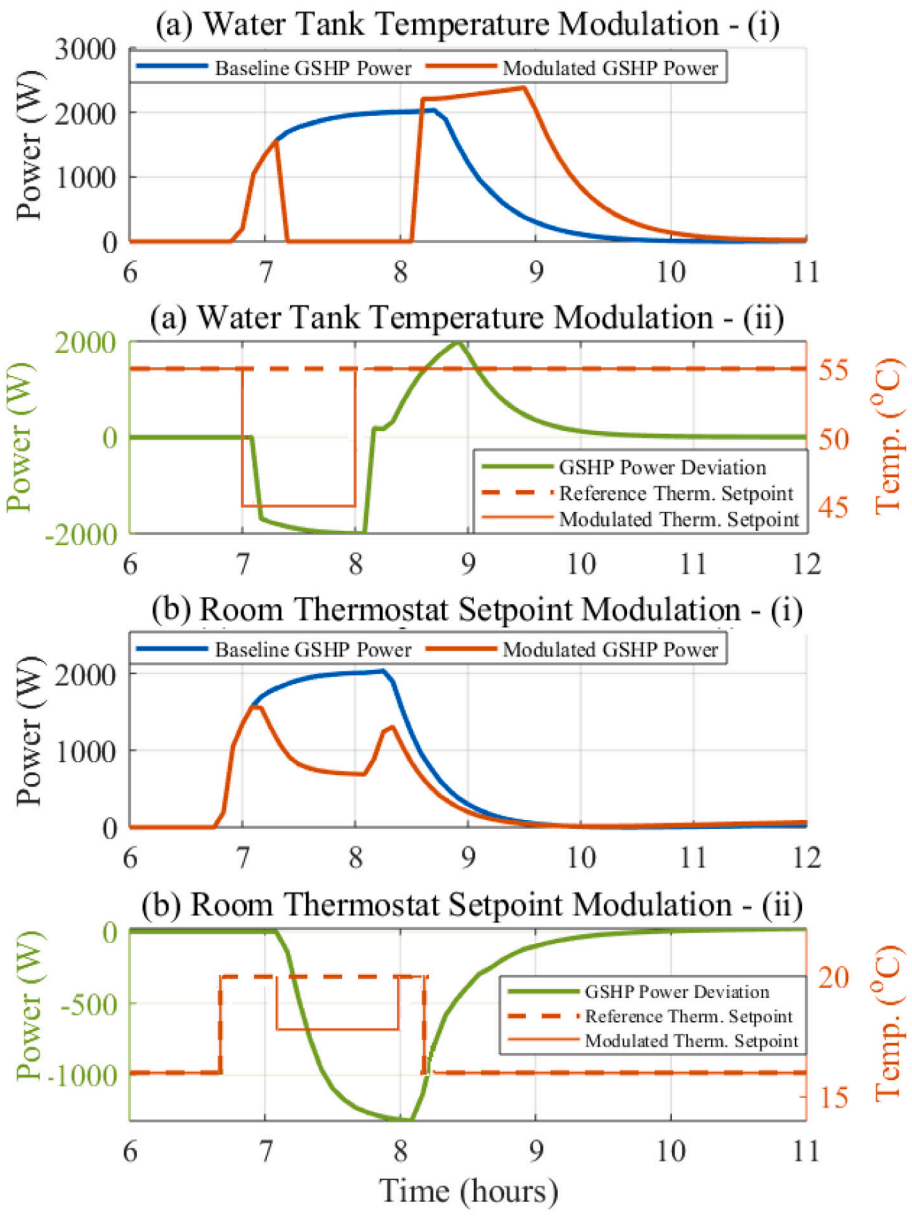

Fig. 9. 1 h down-flex independent DR actions (07:00 to 08:00 h), MH55 case: (a) water tank temperature modulation; (b) room thermostat modulation.

storage capacity is increased by the energy amount resulting from the charging curtailment. Furthermore, the maximum flexibility potential of the EV battery depends not only on the driving patterns but also on the room thermostat setpoint.

The flexibility potential of the active TES, the stationary battery and the EV are all higher for the H55 case because of the higher heat demand. Additionally, zone thermostat setpoints not only influence the GSHP flexibility, but also the electrical storage units flexibility due to their interdependence on the total building load (Eq. (8)).

Fig. 11 shows the storage capacity (C_{DF}) (Eq. (2)) resulting from the activation of the active and passive TES, as well as the exploitation of the stationary battery and the EV, for hourly DR events for the ML55, ML45, L55, L39 cases. A reduced water tank temperature exhibits lower down-flex potential for all systems considered. This is because lower TES tank temperatures result in increased COP and consequently lower GSHP consumption. Overall, the higher the consumption, the higher the associated storage capacity. Furthermore, it can be observed that increased storage capacity is associated with higher thermostatic setpoints, for all considered energy systems.

The storage efficiency (η_{DR}) (Eq. (5)) and self-consumption (SC_{DR}) during a DR action (Eq. (1)), resulting from room and TES tank temperature reductions for all hourly DR events are presented in Fig. 10, both for high heat demand and a reference TES tank temperature of 55 °C (H55 case). In the case of room thermostat modulations, the self-consumption is non-zero for a longer period compared to water tank temperature modulations and it is also maximised earlier (08:00 h–09:00 h) than the PV peak generation period (11:00 h–14:00 h). This is a result of the longer rebounds associated with the activation of the structural TES. In addition, the activation of the passive TES results in less significant rebounds, and thus a greater storage efficiency; however, solar PV generation has a limited effect on the resulting storage efficiency because of the longer duration of the associated rebounds. On the other hand, in case of water tank thermostat modulations, storage efficiency is significantly lower during periods of zero PV electricity generation, since the associated rebounds exhibit greater magnitude. These modulations result in higher self-consumption rates (and storage efficiency) during periods of reduced rebounds (i.e., when the down-flex potential is reduced).

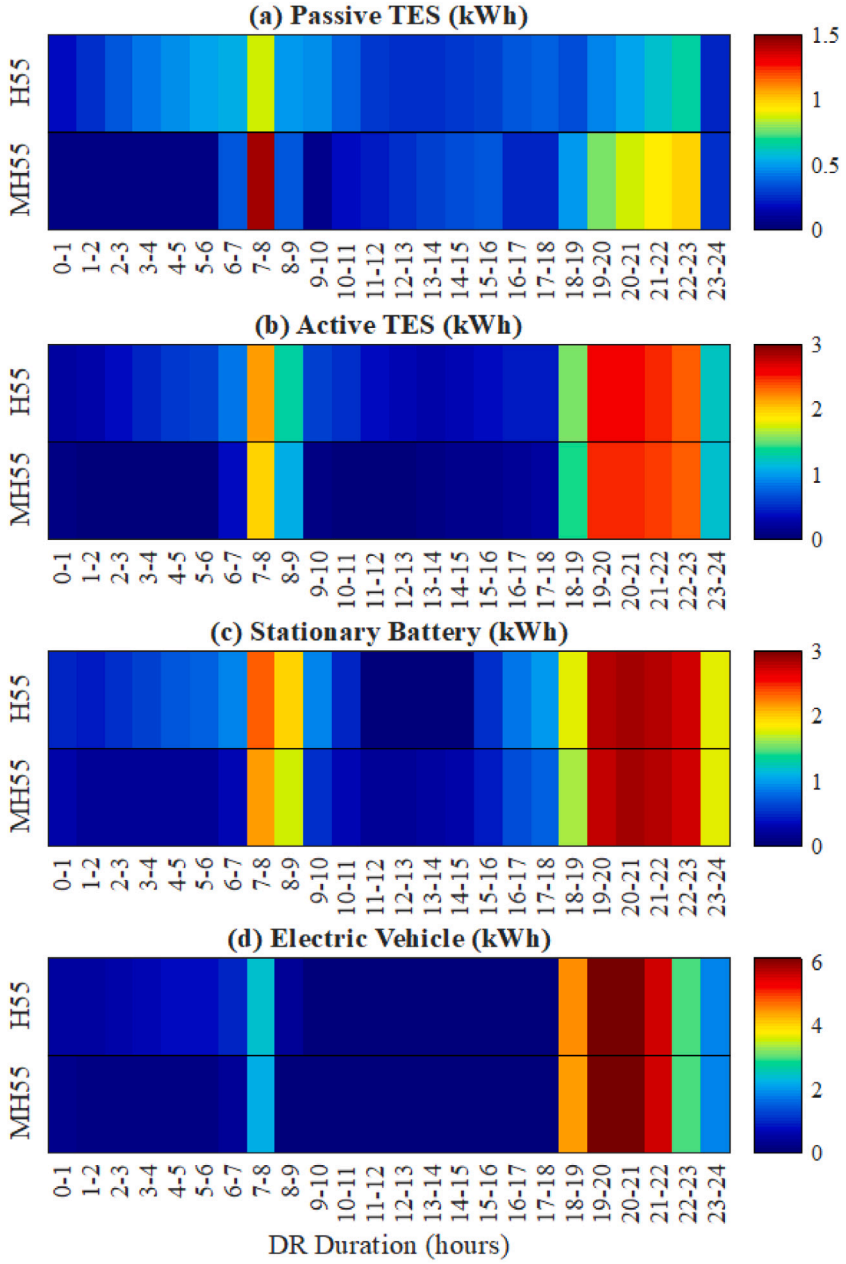

Fig. 10. Storage capacity (C_{DF}) for the H55 and MH55 cases (Hourly down-flex DR actions): (a) passive TES, (b) active TES, (c) stationary battery, and (d) EV.

The storage efficiency mapping provided in Figs. 12 and 13 describe the stationary battery for the H55 and L55 cases, respectively, and provide the storage efficiency for 2 h rebounds occurring up to 15 h after the end of each DR action. Since the storage efficiency (η_{df}) (Eq. (9)) resulting from the use of electrical storage (i.e., the stationary and the EV battery) depends on the rebound starting times (t_c) and rebound duration (η_{id}), each DR action will result in different storage efficiencies for different t_c and τ_{id}. Figs. 13 and 14 (consisting of 16 x 24 tiles) give results based on assessing the storage efficiency resulting from the use of electrical storage for 1 h down-flex demand response events (τ_{rd}=1 h), a rebound duration of 2 h and various rebound commencement time delays (from 0 to 15 h). Accordingly, the X axis corresponds to the time of a given DR event, while the Y axis corresponds to the time (in hours) after which the associated rebound occurs. Thus the tile with $Y = 0$ corresponds to storage efficiencies resulting from rebounds that occur as soon as the DR ends, whereas tiles with $Y = N$ correspond to storage efficiencies resulting from rebounds that occur N h after the end of the DR action, etc. Therefore, the tile with coordinates (2–3, 4) corresponds to the storage efficiency of a 1 h DR action that occurred between 02:00 h and 03:00 h and its associated rebound between 07:00 and 09:00 h .

When solar power is unavailable or less than the building load, the storage efficiency (Eq. (9)) is given by $\eta_{DF} = 1 - 1/\eta_d\eta_c = 1 - 1/0.85^2 = -38.4\%$ and the self-consumption rate (SC_{DR}) is equal to zero. When there is solar energy excess, the storage efficiency (η_{DR}) increases and reaches 100% during high electricity generation periods. The EV battery storage efficiency is constant and equal to: $\eta_{DF} = 1 - 1/0.845^2 = -40.05\%$ as per Eq. (9), since the EV is only plugged in during periods during which local electricity generation is zero. If the EV is plugged-in during periods of onsite electricity generation, its storage efficiency will vary.

In Fig. 13, the dark grey tiles correspond to periods during which no DR actions take place, i.e., when the building load is lower than the PV electricity generation (Eq. (8)). The storage efficiency of DR actions occurring during early hours is higher when the rebound takes

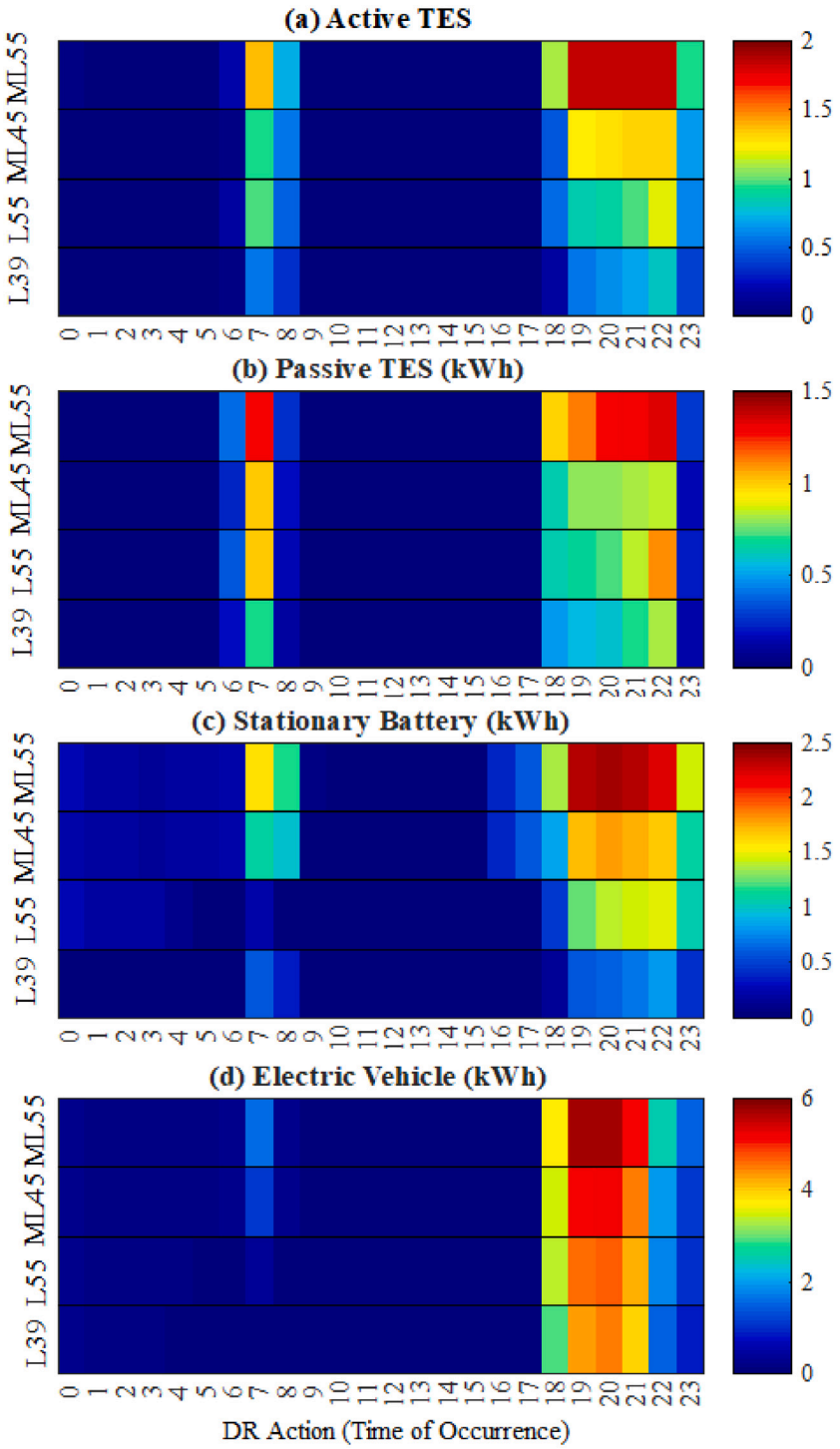

Fig. 11. Storage capacity (C_{DF}) for the ML55, ML45, L55 and L39 cases (Hourly down-flex DR actions): (a) passive TES, (b) active TES, (c) stationary battery, and (d) EV.

place between 10:00 and 14:00 h ; likewise, the storage efficiency of DR actions occurring during evening hours is higher when the rebound takes place the next day. Practically, this flexibility mapping depicts the rationale behind load shifting strategies for solar battery systems; the battery discharges to cover the building demand and charges back later when onsite PV electricity is available.

Comparison of Figs. 13 and 14 show that the stationary battery exhibits higher storage efficiency when the rebound takes place during periods of high onsite electricity generation and low building load, as per Eq. (9). Moreover, the energy flexibility of the stationary battery can be only harnessed when the overall building load is greater than the PV electricity generation. This implies that these periods are limited during days where high PV generation prevails.

4.2. Upward flexibility

To investigate the impact of up-flex actions in terms of their energy shifting capability, energy cost, and coincidence with onsite electricity generation, the notions of storage capacity, C_{UF} (Eq. (4)), storage efficiency, η_{UF} (Eq. (7)), and self-consumption, SC_{DR} (Eq. (1)) are all evaluated, as outlined in Section 2.2. The analysis considers the modulated energy consumption curves and the energy flexibility mappings.

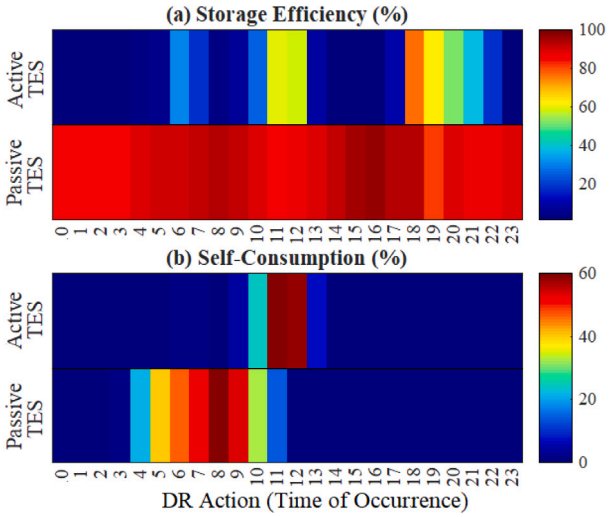

Fig. 12. GSHP (Passive and active TES) (1-hour downward DR actions, H55 case): (a) storage efficiency (η_{DF}) and (b) self-consumption (SC_{DR}).

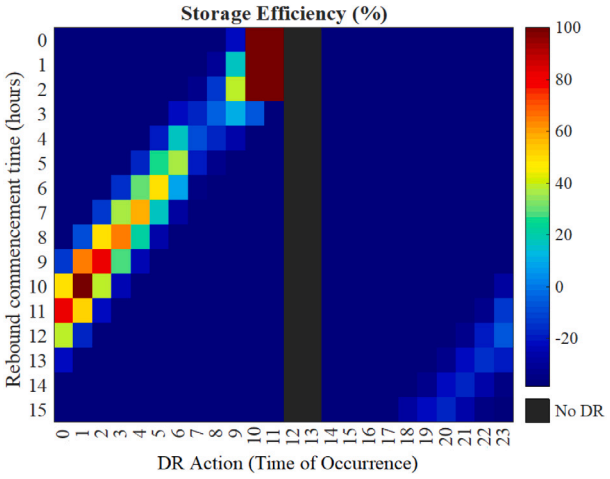

Fig. 13. Storage efficiency (η_{DF}) for the stationary battery, H55 case (1-hour DR down-flex actions): X axis: DR event time. Y axis: Rebound commencement time relative to associated DR action.

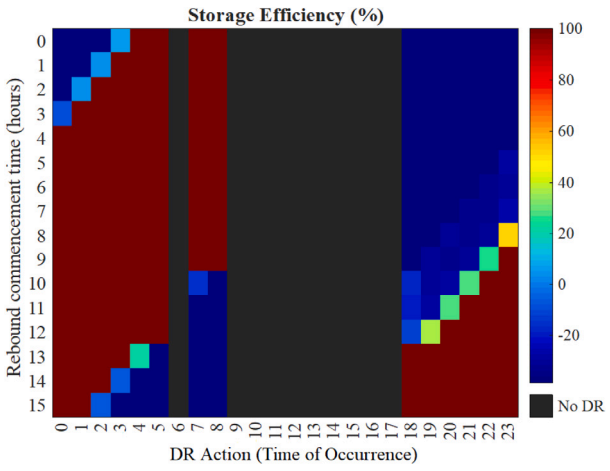

Fig. 14. Storage efficiency (η_{DF}) for the stationary battery, L55 case (1-hour DR down-flex actions): X axis: DR event time. Y axis: Rebound commencement time relative to associated DR action.

4.2.1. Modulated energy consumption curves

The impact of rebounds on the upward flexibility potential is illustrated in Fig. 15 for a one hour demand response event for the GSHP. Modulation occurs at 19:00 h and two separate response profiles are presented. Fig. 15a(i) and (ii) examine the case where the TES tank response (ML45 case) is considered, whereas Fig. 15b(i) and (ii) examine the case where a single zone (living room — see Fig. 4) is analysed. The power deviation curves depicted in Fig. 15a (ii) and b (ii) result from the difference between the baseline and modulated GSHP curves depicted in Fig. 15a(i) and b (i), respectively. This scenario is indicative and is selected to assess the modulated load profile curves resulting from the activation of the passive and active TES at the same time. The activation of the active TES exhibits a significantly higher energy flexibility potential compared to the passive TES activation. It should be noted that the total time of increased demand is substantially different for room thermostat setpoint modulations because of the slower dynamics of the building envelope. Moreover, inverse rebounds resulting from room thermostat setpoint modulations demonstrate a lower magnitude compared to water temperature modulations, however, the latter have significantly lower duration (from 20:10 h to 22:00 h). Thus, the energy savings achieved by implementing water tank temperature upward modulations are significantly higher. It can be observed that up-flex actions for both modulations considered can be covered by local solar power due to the limited time of the DR action (1 h).

An up-flex action is illustrated in Fig. 16 for a one hour water tank temperature modulation between 03:00 and 04:00 for the ML45 case. This scenario corresponds to a water tank preheating strategy during off-peak hours, i.e., when the zone temperature setback is applied. The considered DR action results in two delayed rebounds (see Fig. 16c); this stems from the fact that the thermal energy stored in the water tank during the DR action is consequently used to reduce the GSHP consumption from 0640 to 0820 and delay the evening GSHP activation. This scenario illustrates the GSHP capability to shift rebounds away by combining suitable controls of the room and the water tank temperature setpoint. Accordingly, the two aforementioned thermostat setpoints can be jointly used to control the occurrence time of rebounds and the associated costs.

To study the impact of different baseline water tank temperatures with regard to the activation of the passive TES in up-flex, an upward room thermostat setpoint modulation from 19:00 to 20:00 h for the ML55 and ML45 cases is illustrated in Fig. 17. High baseline water tank temperature modulations result not only in higher storage capacity but also in more significant inverse rebounds.

4.2.2. Energy flexibility maps

The up-flex potential of the GSHP is assessed in Fig. 18 by examining the storage capacity (C_{UF}) (Eq. (3)) of room and water tank thermostatic modulations for all cases considered. During non-occupancy periods, thermal comfort constraints are relaxed additionally as per the ASHRAE guidelines. By comparing the non-activity and non-occupancy periods – which are characterised by the same thermostatic setpoints – it is evident that the relaxation of the boundary conditions results in significantly increased up-flex potential. For example, for case H55 (coldest representative day), the relaxation of thermal constraints results in double storage capacity. For the case L55 (warmest representative day), the storage capacity resulting from hourly DR actions is zero during non-activity periods and 2.2 kWh for non-occupancy periods.

Furthermore, higher reference thermostatic setpoints exhibit lower storage capacity both for room and water tank temperature modulations since during these periods the GSHP reaches its power limits. Similarly, the up-flex potential of lower baseline water tank temperatures is lower for both modulations considered because lower water tank thermostat setpoint temperatures result in lower GSHP capacity. By comparing the storage capacity resulting from the activation of the

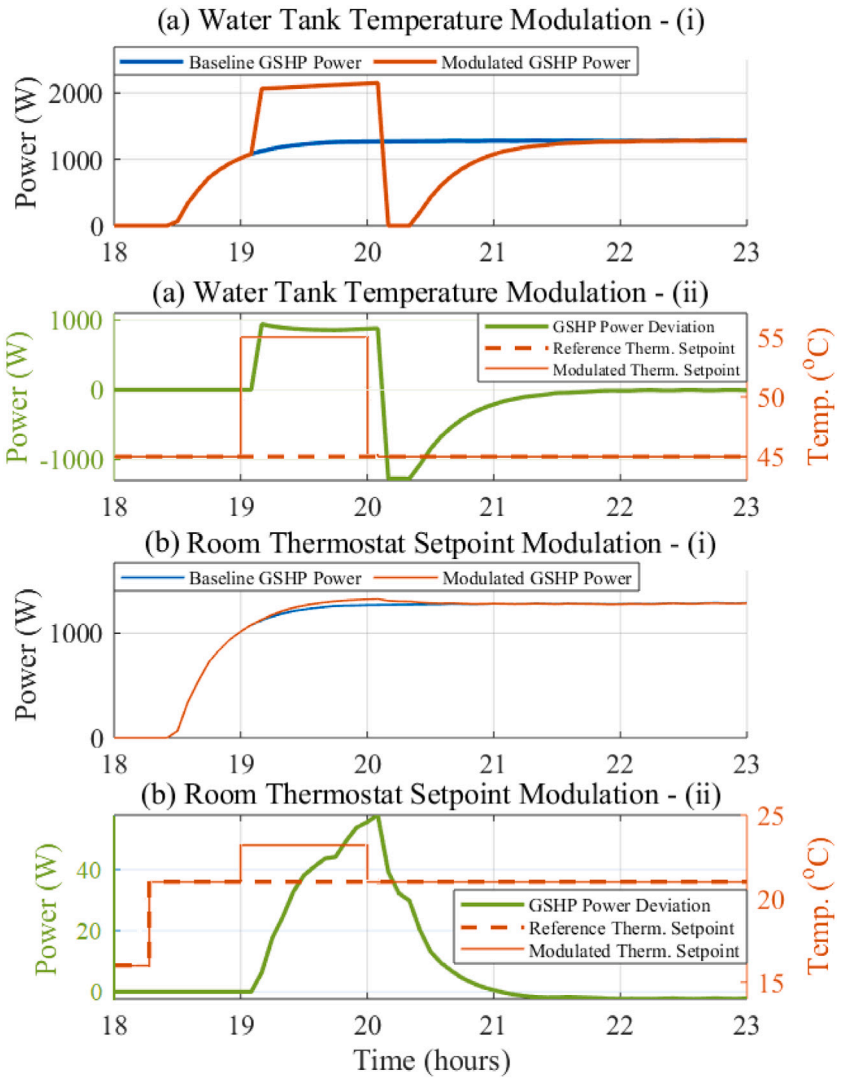

Fig. 15. 1-hour up-flex independent DR actions (19:00 to 20:00 h), ML45 case: (a) water tank temperature modulation; (b) room thermostat modulation.

passive and active TES, it is observed that the up-flex potential of water tank temperature modulations is consistently higher than that of room temperature modulations.

Fig. 19 illustrates the storage efficiency (η_{UF}) (Eq. (6)) and the self-consumption during a DR action (SC_{DR}) (Eq. (1)) for hourly upward modulations of the room and the water tank temperature for the ML45 case. By studying the storage efficiency trends during periods of zero PV generation, it can be observed that the activation of the active TES results in higher storage efficiency compared to that of the passive TES activation; this is due to the higher inverse rebounds resulting from water tank temperature modulations. Both applied modulations exhibit increased storage efficiency during PV generation periods, however, the activation of the passive TES results in lower self-consumption rates (up to 53%). This is due to the fact that the contribution of onsite generation for water tank temperature modulations is lower because of the greater energy volumes resulting from them. On the other hand, room thermostat setpoint modulations can be more effectively covered by onsite electricity generation achieving maximum self-consumption rates equal to 88%.

5. Discussion

Previous research has focused on implicitly assessing building energy flexibility by developing strategies that depend on the underlying algorithms [27] and the market structure [21]. Explicit flexibility evaluation methods that elaborate on diverse flexibility aspects (e.g., energy shifting capability, energy costs, response time recovery period, etc.) have been limited to passive and active TES systems. Few studies [12, 23] evaluate the energy flexibility of both thermal and electrical systems, however, flexibility is assessed at a specific point in time without investigating associated flexibility resulting from later effects. Critically, there is a significant research gap in the literature associated with the integrated flexibility potential of different thermal and electrical systems, the energy costs resulting from harnessing this flexibility as well as the contribution of onsite electricity generation.

To address this gap, a fundamental energy flexibility assessment framework applicable to multicomponent thermal and electrical systems commonly found in residential buildings has been developed in the current work. The proposed methodology can capture the DR potential of a building and depict it in a concise and consistent manner. The daily flexibility analysis and associated mappings illustrate the energy shifting capability of different energy storage units, as well as the associated energy costs. Interestingly, these indicators not only provide information about the energy-related flexibility potential but also give insights into qualitative characteristics of electricity consumption during DR actions. For example, for down-flex, non-zero self-consumption rates during periods of onsite generation, non-availability is associated with protracted rebounds. Simulation results have shown that

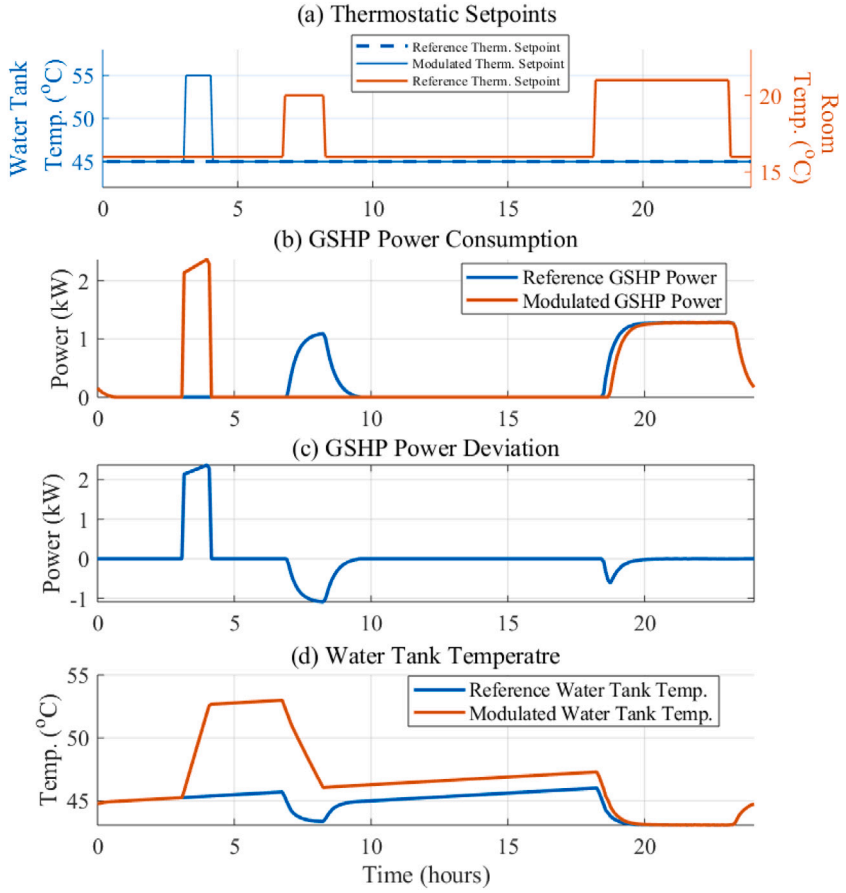

Fig. 16. Up-flex DR action between 03:00 and 04:00, water tank temperature modulation,ML45 case: (a) room and water tank thermostatic setpoints, (b) GSHP power consumption (c) GSHP power deviation, (d) water tank temperature.

higher baseline water tank temperatures result in higher electricity consumption (due to the GSHP COP) and higher storage capacity, both in down-flex and up-flex scenarios. In addition, water tank and room temperature modulations, if combined, can shift rebound occurrences away from peak demand periods or periods of low onsite electricity generation. Furthermore, rebounds related to downward room temperature modulations have a longer duration thus limiting the contribution of locally produced electricity. Rebounds related to water tank temperature modulations, in contrast, have a shorter duration thus allowing for better coincidence with onsite PV generation. Moreover, up-flex actions for both considered modulations can be more effectively covered by local solar power due to the possibility to control the time and duration of increased demand during a DR action. The up-flex potential of the building structural TES can be significantly increased when thermal comfort constraints are relaxed beyond normal limits.

The obtained flexibility maps depend on the building model utilised in the current study as well as the utilised occupancy profiles. For instance, the characteristics of the building thermal envelope, and the heating system specifications determine the dynamics of the modulated power demand during DR actions and hence the resulting energy consumption and associated energy costs. The associated results have shown that occupant preferences may play a key role in shaping the building electricity profile, both for the reference case scenarios and the periods of modulated power demand. These preferences determine the thermostatic setpoints, the consumption of non-controllable loads, and the EV driving schedule and the resulting flexibility potential. For example, the EV battery flexibility is determined not only by the occupant driving patterns but also by the heating system (GSHP) performance and the building load itself. This implies that the energy flexibility potential of a building is determined by weather and occupant thermal

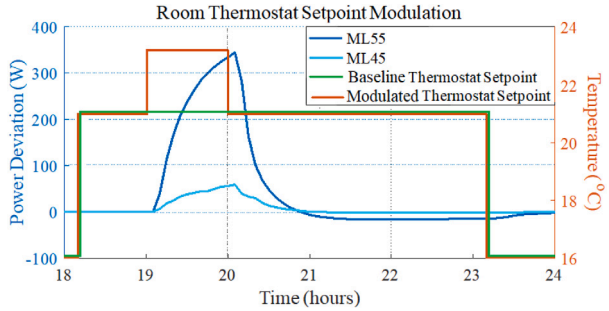

Fig. 17. Up-flex DR action between 19:00 and 20:00, zone thermostat setpoint, H55 and H45 cases.

comfort preferences as well as the use of appliances, lighting, etc. The flexibility margin of the various DR scenarios associated with the heating system is affected by the maximum allowable operative temperature drifts. Although the allowable temperature drifts were determined in the current work as per ASHRAE standards [41], the adopted thermal comfort constraints are likely to vary depending on the occupant thermal comfort preferences. In addition, the net energy cost of harnessing the flexibility potential of the active and passive TES is influenced by the power consumption curve of the non-controllable loads. This stems from the dependency of the storage efficiency (Eqs. (5)–(6)) and self-consumption rates (Eq. (1)) on the total building load.

The presented methodology is capable of being applied to other buildings which include electric heating systems, hot water TES, electrical energy storage, and electric vehicles (provided that a control

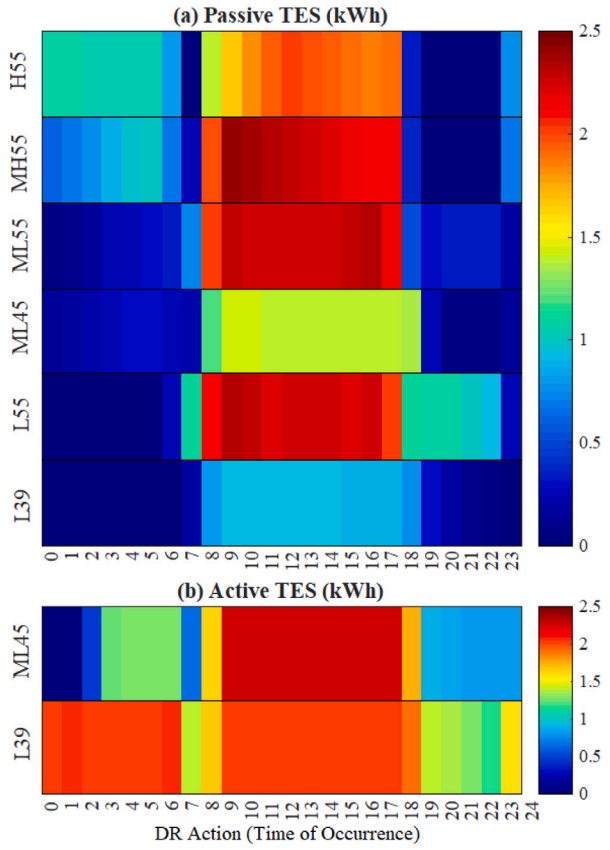

Fig. 18. Storage capacity (C_{UF}), hourly up-flex DR actions for the ML55, ML45, L55, and L39 cases (Hourly up-flex DR actions): (a) passive TES, (b) active TES.

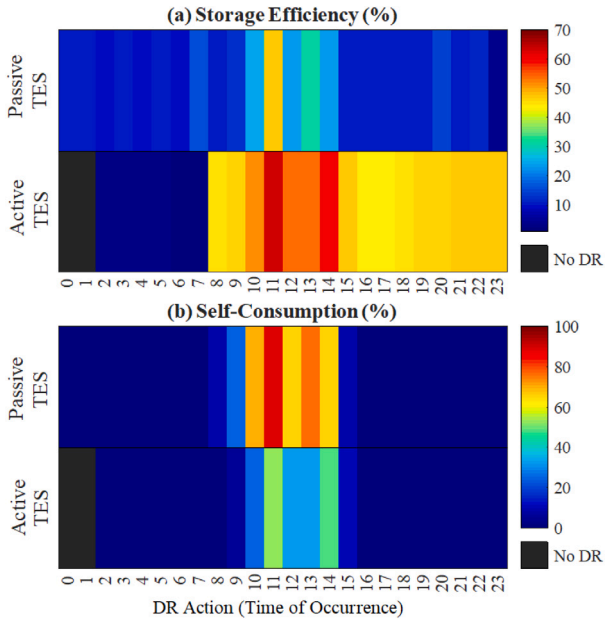

Fig. 19. GSHP (passive and active TES) (1-hour upward DR actions, L39 case): (a) storage efficiency η_{UF} and (b) self-consumption (SC_{DR}).

setpoint can be used) as well as locally produced electricity. However, the obtained results assume a single baseline consumption curve for each case under study. This follows from the fact that all applied DR actions are independent, and every next DR action is not affected by the previous ones. In a practical application of these indicators, the intervals between DR actions must be long enough (so that the resulting rebounds will not affect the following DR actions) or the reference case must be readjusted for the following DR action. Furthermore, hot water TES systems may be found in different configurations (coupled with domestic hot water and/or heating systems) depending on the considered building instance. The DR actions related to them may influence thermal comfort, as the associated constraints depend on the characteristics of the HVAC system. This indicates that the corresponding boundary conditions determination is case specific and that the proposed methodology should be suitably adapted according to the TES system configuration.

Each energy flexibility indicator can be used in different stages of the building energy flexibility characterisation process by serving various objectives. The storage capacity (Eqs. (2) & (4)) gives insights not only into the energy volumes that can be shifted but also into the periods during which these volumes can be dispatched. Furthermore, storage efficiency (Eqs. (5) & (6)) can be used to assess the rebounds resulting from the heating system flexibility exploitation which are likely to create peaks comparable to the building baseline operation. On the other hand, the self-consumption (Eq. (1)) during a DR action is a measure of its environmental impact and can be used by aggregators to optimise building performance against CO_2 emission targets. Similarly, each energy system exhibits diverse characteristics during a DR action. For instance, the building structural TES exhibits lower down-flex potential and increased storage efficiency compared to the active TES because of its dependence on thermal comfort constraints and lower rebounds. Moreover, the self-consumption exhibited by the passive TES is maximised earlier than that of the active TES. Therefore, the optimal flexibility potential exploitation of each energy system along with the prioritisation of the flexibility indicator used depends on the external environment (including energy grids, RES, etc.), occupant lifestyle, and optimisation objectives of the aggregator portfolio.

The proposed flexibility indicators depend on both the reference and modulated power consumption data as well as the electricity production data from the local PV power plant. The building model predictions and thereby the applied modulations were validated against measured data from the existing building. Specifically, the building model and all associated components (thermal envelope, HVAC system, PV system, EV) were modelled using EnergyPlus V.9.1 and calibrated against experimental data from the building according to ASHRAE calibration guidelines [45]. The building model accuracy was evaluated by using the Mean Bias Error [46] and the Cumulative Variation Root Mean Squared Error based on the specification of the annual error against one year of collected data (2012).

To quantify the building energy flexibility potential, both the reference (P_{ref}) and the modulated (P_{mod}) building load should be determined. In the literature, the building flexibility potential has been evaluated by using either offline system modelling (white-box [18] and grey-box models [16]) or data-driven approaches [33] based on available sensor data.based on available sensor data. In this study, both the reference and modulated consumption curves have been acquired using a white-box model calibrated against measured data from the building. For the practical application of the proposed methodology, one possible approach is the use of a statistical time series analysis to determine P_{ref}. Thus, it is necessary to follow a data-driven modelling approach considering continual training by using incoming smart metre data. Future work will extend this white-box model methodology to evaluate residential building energy flexibility in a dynamic environment by using machine learning techniques.

6. Conclusions and future work

In this paper, a generic energy flexibility quantification framework has been presented to characterise the DR potential of the most common energy systems found in residential buildings. Specifically, the

flexibility potential of the building structural thermal mass, the hot water tank thermal energy storage, and the electrical energy storage units are evaluated by using the proposed indicators — namely storage capacity, storage efficiency, and self-consumption during a DR action. This methodology has the potential to be applied to all residential building types, depict the DR potential of individual power modulation strategies, and finally illustrate it in a succinct and uniform way. Building owners can benefit from this framework by allowing them to assess flexibility programmes, while aggregators can evaluate all possible flexibility measure combinations, in conjunction with the associated costs as well as grid integration issues, and eventually optimise building portfolios with which to contract. Simulation results have shown that higher baseline water tank temperatures result in higher storage capacity, both for downward and upward regulation. Furthermore, the combined modulation of the water tank and room thermostats can shift rebounds away from peak demand periods or periods of low onsite electricity generation. Moreover, up-flex actions associated with the activation of the active and passive thermal energy storage can be more effectively covered by local solar power due to the possibility to control the time and duration of increased demand during a DR action. In addition, the relaxation of thermal comfort constraints beyond normal limits results in increased up-flex potential of the building structural thermal energy storage, while water tank thermostat modulations have a minor impact on thermal comfort. Finally, it is demonstrated that the procured flexibility of each system is a multivariate attribute which depends on weather conditions, occupant lifestyle as well as the energy consumption of the various systems of the installation.

Nomenclature

Symbol	Definition
t_{DR}	Duration of DR Event (hours)
τ_{rd}	Total time of reduced demand (hours)
τ_{id}	Total time of increased demand (hours)
SC_{DR}	Self-consumption during a DR action (adim)
P_{mod}	Modulated building load (W)
P_{ref}	Reference building load (W)
P_{RES}	Onsite electricity generation (W)
C_{DR}	Available storage capacity (kWh)
C_{DF}	Available storage capacity in down-flex (kWh)
C_{UF}	Available storage capacity in up-flex (kWh)
η_{DF}	Storage Efficiency in down-flex (adim)
η_{DF}	Storage Efficiency in up-flex (adim)
ΔT_r	Room thermostat setpoint modulation (K)
ΔT_{wt}	Water tank thermostat setpoint modulation (K)
SoC_{ref}	Reference SoC (adim)
P_b	Building Load (W)
η_d	Battery discharging efficiency (adim)
η_c	Battery charging efficiency (adim)
t_c	Rebound commencement time (hours)
T_r	Zone thermostat setpoint (°C)
T_{wt}	Water tank temperature setpoint (°C)
$T_{wt,min}$	Minimum storage tank temperature for which thermal comfort conditions can be maintained (°C)

Abbreviation	Definition
RES	Renewable Energy Sources
DSF	Demand Side Flexibility
DR	Demand Response
HP	Heat Pump
HVAC	Heat, Ventilation, and Air Conditioning
TES	Thermal Energy Storage
EV	Electric Vehicle
SoC	State of Charge
MBE	Mean Bias Error
CVRMSE	Cumulative Variation Root Mean Error
GSHP	Ground Source Hear Pump
COP	Coefficient of Performance

CRediT authorship contribution statement

Adamantios Bampoulas: Conceptualization, Methodology, Validation, Formal analysis, Writing - original draft, Writing - review & editing, Visualization, Project administration. **Mohammad Saffari:** Conceptualization, Writing - review & editing, Supervision. **Fabiano Pallonetto:** Conceptualization, Writing - review & editing, Supervision. **Eleni Mangina:** Conceptualization, Writing - review & editing, Funding acquisition, Project administration, Supervision. **Donal P. Finn:** Conceptualization, Writing - review & editing, Funding acquisition, Project administration, Supervision.

Declaration of competing interest

The authors declare that they have no known competing financial interests or personal relationships that could have appeared to influence the work reported in this paper.

Acknowledgements

This work has emanated from research conducted with the financial support of Science Foundation Ireland under the SFI Strategic Partnership Programme Grant Number SFI/15/SPP/E3125 and additional funding provided by the UCD Energy Institute. The opinions, findings and conclusions or recommendations expressed in this material are those of the authors and do not necessarily reflect the views of the Science Foundation Ireland.

Appendix

During the rebound, the modulated building power is equal to $P_{mod} = P_b + P'$, where P' the additional power needed to restore the battery SoC. Assuming that the rebound duration, τ_{id} is adequate to restore the battery SoC and P' lies in acceptable limits according to the electrical storage system specifications, then $\int_{t_c}^{t_c+\tau_{id}} P'dt = C_{DF}/\eta_c\eta_d$. Eq. (5) can be written as follows:

$$\eta_{DF} = 1 - \frac{\int_0^{\infty} \max(P_{\mathrm{mod}} - \max(P_{ref}, P_{RES}), 0)dt}{\int_0^{\infty} |(P_{\mathrm{mod}} - P_{ref})^-|dt} =$$
$$= 1 - \frac{\int_0^{t_{dr}} \max(0 - \max(\max(P_b - P_{RES}, 0), P_{RES}), 0)dt + \int_{t_c}^{t_c+\tau_{id}} \max(P_b + P' - \max(P_b, P_{RES}), 0)dt}{C_{DF}} =$$
$$= 1 - \frac{\int_{t_c}^{t_c+\tau_{id}} \max(P_b + P' - \max(P_b, P_{RES}), 0)dt}{C_{DF}} =$$
$$= 1 - \frac{\max(\int_{t_c}^{t_c+\tau_{id}} P' + P_b - \max(P_b, P_{RES})dt, 0)}{C_{DF}} =$$
$$= 1 - \frac{\max(\int_{t_c}^{t_c+\tau_{id}} P'dt + \int_{t_c}^{t_c+\tau_{id}} P_b - \max(P_b, P_{RES})dt, 0)}{C_{DF}} =$$
$$= 1 - \frac{\max(C_{DF}/\eta_c\eta_d + \int_{t_c}^{t_c+\tau_{id}} P_b - \max(P_b, P_{RES})dt, 0)}{C_{DF}} =$$
$$= 1 - \frac{\max(C_{DF}/\eta_c\eta_d + \int_{t_c}^{t_c+\tau_{id}} P_b - \max(P_b, P_{RES})dt, 0)}{C_{DF}} =$$
$$= 1 - \max(\frac{1}{\eta_c\eta_d} - \frac{\int_{t_c}^{t_c+\tau_{id}} \max(P_b, P_{RES})dt, 0 - P_b}{C_{DF}}, 0)$$
$$= 1 - \max(\frac{1}{\eta_c\eta_d} - \frac{1}{C_{DF}} \int_{t_c}^{t_c+\tau_{id}} \max(P_b, P_{RES}) - P_b dt, 0)$$

References

[1] Impact Assessment study on downstream flexibility, price flexibility, demand response and smart metering. Brussels, Belgium: European Commission DG Energy; 2016.
[2] CEER advice on ensuring market and regulatory arrangements help deliver demand-side flexibility. CEER (Council of European Energy Regulators); 2014.
[3] Explicit demand response in europe, mapping the markets. Smart Energy Demand Coalition (SEDC); 2017.

[4] Directive (EU) 2018/2001 of the European parliament and of the Council of 11 December 2018 on the promotion of the use of energy from renewable sources. Off J Eur Union 2018.

[5] Economidou M, Laustsen J, Ruyssevelt P, Staniaszek D. Europe's Buildings under the Microscope, A country-by-country review of the energy. Buildings Performance Institute Europe; 2011.

[6] Li PH, Pye S. Assessing the benefits of demand-side flexibility in residential and transport sectors from an integrated energy systems perspective. Appl Energy 2018;228:965–79. http://dx.doi.org/10.1016/j.apenergy.2018.06.153.

[7] Jensen SO, Madsen H, Lopes R, Junker RG, Aelenei D, Li R, et al. Energy flexibility as a key asset in a smart building future. 2017.

[8] Jensen SO, Marszal-Pomianowska A, Lollini R, Pasut W, Knotzer A, Engelmann P, et al. IEA EBC Annex 67 energy flexible buildings. Energy Build 2017;155:25–34. http://dx.doi.org/10.1016/j.enbuild.2017.08.044.

[9] Junker RG, Azar AG, Lopes RA, Lindberg KB, Reynders G, Relan R, et al. Characterizing the energy flexibility of buildings and districts. Appl Energy 2018;225:175–82. http://dx.doi.org/10.1016/j.apenergy.2018.05.037.

[10] Hewitt NJ. Heat pumps and energy storage – The challenges of implementation. Appl Energy 2012;89:37–44. http://dx.doi.org/10.1016/j.apenergy.2010.12.028.

[11] Arteconi A, Costola D, Hoes P, Hensen JLM. Analysis of control strategies for thermally activated building systems under demand side management mechanisms. Energy Build 2014;80:384–93. http://dx.doi.org/10.1016/j.enbuild.2014.05.053.

[12] D'hulst R, Labeeuw W, Beusen B, Claessens S, Deconinck G, Vanthournout K. Demand response flexibility and flexibility potential of residential smart appliances: Experiences from large pilot test in Belgium. Appl Energy 2015;155:79–90. http://dx.doi.org/10.1016/j.apenergy.2015.05.101.

[13] Nuytten T, Claessens B, Paredis K, Bael JV, Six D. Flexibility of a combined heat and power system with thermal energy storage for district heating. Appl Energy 2013;104:583–91. http://dx.doi.org/10.1016/j.apenergy.2012.11.029.

[14] Six D, Desmedt J, Vanhoudt D, Bael JV. Exploring the flexibility potential of residential heat pumps combined with thermal energy storage for smart grids. In: 21st international conference on electricity distribution; 2011.

[15] Tahersima F, Stoustrup J, Meybodi SA, Rasmussen H. Contribution of domestic heating systems to smart grid control. In: IEEE conference on decision and control and European control conference, Orlando, FL, USA. 2011, p. 3677–81. http://dx.doi.org/10.1109/CDC.2011.6160913.

[16] Reynders G, Diriken J, Saelens D. Generic characterization method for energy flexibility: Applied to structural thermal storage in residential buildings. Appl Energy 2017;198:192–202. http://dx.doi.org/10.1016/j.apenergy.2017.04.061.

[17] Foteinaki K, Rongling L, Heller A, Rode C. Heating system energy flexibility of low-energy residential buildings. Energy Build 2018;180. http://dx.doi.org/10.1016/j.enbuild.2018.09.030.

[18] Dréau JL, Heiselberg P. Energy flexibility of residential buildings using short term heat storage in the thermal mass. Energy 2016;111:991–1002. http://dx.doi.org/10.1016/j.energy.2016.05.076.

[19] Foteinaki K, Li R, Péan T, Rode C, Salom J. Evaluation of energy flexibility of low-energy residential buildings connected to district heating. Energy Build 2020;213. http://dx.doi.org/10.1016/j.enbuild.2020.109804.

[20] Masy G, Georges E, Verhelst C, Lemort V, André P. Smart grid energy flexible buildings through the use of heat pumps and building thermal mass as energy storage in the Belgian context. Sci Technol Built Environ 2015;21:800–11. http://dx.doi.org/10.1080/23744731.2015.1035590.

[21] Kathirgamanathan A, Péan T, Zhange K, Rosa MD, Salom J, Kummert M, et al. Towards standardising market-independent indicators for quantifying energy flexibility in buildings. Energy Build 2020;220. http://dx.doi.org/10.1016/j.enbuild.2020.110027.

[22] Finck C, Lib R, Kramer R, Zeilera W. Quantifying demand flexibility of power-to-heat and thermal energy storage in the control of building heating systems. Appl Energy 2018;209:409–25. http://dx.doi.org/10.1016/j.apenergy.2017.11.036.

[23] Zhou Y, Cao S. Quantification of energy flexibility of residential net-zero-energy buildings involved with dynamic operations of hybrid energy storages and diversified energy conversion strategies. Sustain Energy Grids Netw 2020;21. http://dx.doi.org/10.1016/j.segan.2020.100304.

[24] Pallonetto F, Rosa MD, D'Ettorre F, Finn DP. On the assessment and control optimisation of demand response programs in residential buildings. Renew Sustain Energy Rev 2020;127:109861. http://dx.doi.org/10.1016/j.rser.2020.109861.

[25] Mirakhorli A, Dong B. Market and behavior driven predictive energy management for residential buildings. Sustainable Cities Soc 2018;38:723–35. http://dx.doi.org/10.1016/j.scs.2018.01.030.

[26] Shafie-Khah M, Siano P. A stochastic home energy management system considering satisfaction cost and response fatigue. IEEE Trans Ind Inf 2018;14(2):629–38. http://dx.doi.org/10.1109/TII.2017.2728803.

[27] Reynders G, Lopes RA, Marszal-Pomianowska A, Aelenei D, Martins J, Saelens D. Energy flexible buildings: An evaluation of definitions and quantification methodologies applied to thermal storage. Energy Build 2018;166:372–90. http://dx.doi.org/10.1016/j.enbuild.2018.02.040.

[28] Coninck RD, Helsen L. Quantification of flexibility in buildings by cost curves – Methodology and application. Appl Energy 2016;162:653–65. http://dx.doi.org/10.1016/j.apenergy.2015.10.114.

[29] Péan TQ, Torres B, Salom J, Ortiz J. Representation of daily profiles of building energy flexibility. In: Sim IBPSA conference. Montreal, Canada; 2018.

[30] Rodríguez LR, Ramos JS, Álvarez Domínguez S, Eicker U. Contributions of heat pumps to demand response: A case study of a plus-energy dwelling. Appl Energy 2018;214:191–204. http://dx.doi.org/10.1016/j.apenergy.2018.01.086.

[31] Kelly NJ, Tuohy PG, Hawkes AD. Performance assessment of tariff-based air source heat pump load shifting in a UK detached dwelling featuring phase change-enhanced buffering. Appl Therm Eng 2014;71(2):809–20. http://dx.doi.org/10.1016/j.applthermaleng.2013.12.019.

[32] Baeten B, Rogiers F, Helsen L. Reduction of heat pump induced peak electricity use and required generation capacity through thermal energy storage and demand response. Appl Energy 2017;195:184–95. http://dx.doi.org/10.1016/j.apenergy.2017.03.055.

[33] Balint A, Kazmi H. Determinants of energy flexibility in residential hot water systems. Energy Build 2019;188–189:286–96. http://dx.doi.org/10.1016/j.enbuild.2019.02.016.

[34] Stinner S, Huchtemann K, Müller D. Quantifying the operational flexibility of building energy systems with thermal energy storages. Appl Energy 2016;181:140–54. http://dx.doi.org/10.1016/j.apenergy.2016.08.055.

[35] Barelli L, Bidini G, Bonucci F, Ottaviano A. Residential micro-grid load management through artificial neural networks. J Energy Storage 2018;17:287–98. http://dx.doi.org/10.1016/j.est.2018.03.011.

[36] Shahgoshtasbi D, Jamshidi MM. A new intelligent neuro–fuzzy paradigm for energy-efficient homes. IEEE Syst J 2014;8:664–73. http://dx.doi.org/10.1109/JSYST.2013.2291943.

[37] Brahman F, Honarmand M, Jadid S. Optimal electrical and thermal energy management of a residential energy hub, integrating demand response and energy storage system. Energy Build 2015;90:65–75. http://dx.doi.org/10.1016/j.enbuild.2014.12.039.

[38] Alirezaei M, Noori M, Tatari O. Getting to net zero energy building: Investigating the role of vehicle to home technology. Energy Build 2016;130:465–76. http://dx.doi.org/10.1016/j.enbuild.2016.08.044.

[39] International Energy Agency. Examples of energy flexibility in buildings. 2019, http://www.annex67.org/media/1894/examples-of-energy-flexibility-in-buildings.pdf.

[40] Mazzi PPN. Wind power in electricity markets and the value of forecasting. In: Renewable energy forecasting. Woodhead publishing series in energy, Woodhead Publishing; 2017, p. 259–78. http://dx.doi.org/10.1016/B978-0-08-100504-0.00010-X.

[41] Thermal environmental conditions for human occupancy. 2017, ANSI/ASHRAE Standard 55-2017.

[42] Mullan J, Harries D, Bräunl T, Whitely S. The technical, economic and commercial viability of the vehicle-to-grid concept. Energy Policy 2012;48:394–406. http://dx.doi.org/10.1016/j.enpol.2012.05.042.

[43] Pallonetto F, Mangina E, Milano F, Finn D. SimApi, a smartgrid co-simulation software platform for benchmarking building control algorithms. SoftwareX 2019;9:271–81. http://dx.doi.org/10.1016/j.softx.2019.03.003.

[44] EnergyPlusversion 9.1. Big Ladder Software, [Online]. https://bigladdersoftware.com/epx/docs/9-1/.

[45] Measurement of energy, demand, and water savings. ASHRAE Guideline 14-2014.

[46] Mustafaraj G, Marini D, Costa A, Keane M. Model calibration for building energy efficiency simulation. Appl Energy 2014;130:72–85. http://dx.doi.org/10.1016/j.apenergy.2014.05.019.

[47] Pallonetto F, Mangina E, Finn D, Wang F, Wang A. A restful API to control a energy plus smart grid-ready residential building: Demo abstract. In: Proceedings of the 1st ACM Conference on embedded systems for energy-efficient buildings. BuildSys '14, New York, NY, USA: Association for Computing Machinery; 2014, p. 180–1. http://dx.doi.org/10.1145/2674061.2675023.

[48] Ireland Central Statistics Office. The roof over our heads. 2011, URL http://www.cso.ie.

[49] Pallonetto F, Rosa MD, Finn DP. Environmental and economic benefits of building retrofit measures for the residential sector by utilizing sensor data and advanced calibrated models. Adv Build Energy Res 2020;1–29. http://dx.doi.org/10.1080/17512549.2020.1801504.

[50] Coakley D. Calibration of detailed building energy simulation models to measured data using uncertainty analysis [Ph.D. thesis], University of Cork; 2014.

[51] Pallonetto F, Oxizidis S, Milano F, Finn DP. Model calibration for building energy efficiency simulation. Energy Build 2016;130:72–85. http://dx.doi.org/10.1016/j.apenergy.2014.05.019.

[52] Buttitta G, Turner WJN, Neu O, Finn DP. Development of occupancy-integrated archetypes: Use of data mining clustering techniques to embed occupant behaviour profiles in archetypes. Energy Build 2019;198:84–99. http://dx.doi.org/10.1016/j.enbuild.2019.05.056.

[53] Buttitta G, Finn DP. A high-temporal resolution residential building occupancy model to generate high-temporal resolution heating load profiles of occupancy-integrated archetypes. Energy Build 2020;206. http://dx.doi.org/10.1016/j.enbuild.2019.109577.

[54] Masoum AS, Deilami S, Moses PS, Abu-Siada A. Impacts of battery charging rates of plug-in electric vehicle on smart grid distribution systems. In: IEEE PES innovative smart grid technologies conference Europe (ISGT Europe), Gothenberg, Sweden. 2010, http://dx.doi.org/10.1109/ISGTEUROPE.2010.5638981.

[55] McInerney T, Vermette S. Development of a severe winter index: Buffalo, New York. Geogr Bull 2008;49:47–55.

[56] Mourshed M. Relationship between annual mean temperature and degree-days. Energy Build 2012;54:418–25. http://dx.doi.org/10.1016/j.enbuild.2012.07.024.